SUPPLEMENTARY INFORMATION

A photosynthetic alveolate closely related to apicomplexan parasites

Robert B. Moore*[1,2], Miroslav Oborník*[3], Jan Janouškovec[3], Tomáš Chrudimský[3], Marie Vancová[3], David H. Green[4], Simon W. Wright[5], Noel W. Davies[6], Christopher J.S. Bolch[7], Kirsten Heimann[8], Jan Šlapeta[9], Ove Hoegh-Guldberg[10], John M. Logsdon Jr[2], Dee A. Carter[1§].

[1]School of Molecular and Microbial Biosciences, University of Sydney, Darlington, NSW 2006 Australia. [2]Roy J. Carver Center for Comparative Genomics, Department of Biological Sciences, University of Iowa, Iowa City, IA 52242-1324 USA. [3]Biology Centre of the Academy of Sciences of the Czech Republic, Institute of Parasitology, and University of South Bohemia, Faculty of Science, Branišovská 31, 37005 České Budějovice, Czech Republic. [4]Scottish Association for Marine Science, Dunstaffnage Marine Laboratory, Oban, Argyll, PA37 1QA UK. [5]Australian Antarctic Division, Kingston, Tasmania 7050 Australia. [6]Central Science Laboratory, University of Tasmania, Hobart, Tasmania 7001 Australia. [7]School of Aquaculture, University of Tasmania, Launceston, Tasmania 7250 Australia. [8]School of Marine and Tropical Biology, James Cook University, Townsville, Qld 4811 Australia. [9]Faculty of Veterinary Science, University of Sydney, Sydney, NSW 2006 Australia. [10]Centre for Marine Studies, University of Queensland, St Lucia, Qld 4072 Australia.

[§]Corresponding author (d.carter@mmb.usyd.edu.au).

*These authors contributed equally to this work.

Sections:

1. Taxonomy of *Chromera velia* ..... page 1
2. Isolation and culturing of *C. velia* 2
3. DNA extraction 4
4. PCR of genes for phylogeny and confirmation of culture purity 4
5. Phylogenetic analyses 5
6. Pigment analysis and photosynthesis 8
7. Light microscopy 11
8. Fluorescence microscopy 11
9. Electron microscopy 12

1. Taxonomy of *Chromera velia*

The name *Chromera velia* is formally introduced according to the International Code of Zoological Nomenclature[1]. The genus name is not treated as a Latin or Greek word. The genus nomenclature is influenced by observations of the chromophores (pigmentation) of the meront (division products).

The name *Chromera* reflects that in pure culture the pigmented plastid is inherited through cell division over many years. i.e. the plastid is not a kleptoplastid. We define the gender of genus *Chromera* as feminine. The entire generic name is the stem. The species epithet refers to the rarity of observation of the flagellate life-stage. The species epithet is feminine.

The hapantotype and cultures were processed and submitted under the culture code RM12, which is the original strain identifier (R. Moore, 2006, University of Sydney, PhD thesis).

Phylum Chromerida belongs to Alveolata sensu Adl *et al.* 2005[2]. Chromerids contain a photosynthetic secondary plastid, bearing chlorophyll *a* but no chlorophyll c. The phylum currently comprises a single species *Chromera velia*.

Chromera is clearly an alveolate, but is also unique and novel because it differs from all other alveolates. It differs from Colpodellida[3,4] (Cavalier Smith 1993) Conoidasida[5] (Levine 1988), Aconoidasida[6] (Mehlhorn *et al.* 1980), Perkinsidae[7,2] (Levine 1978, emend. Adl *et al*. 2005), Oxyrrhia[8] (Cavalier-Smith and Chao 2004), Ciliophora[9,8,10] (Doflein, 1901), Ellobiopsea[3,11,8] (Cavalier Smith 1993) and Colponemea[3,8] (Cavalier-Smith 1993, emend Cavalier-Smith and Chao 2004) in that it contains a heritable photosynthetic plastid while they do not. It differs from Dinoflagellata[12,13] (Bütschli, 1885, emend. Fensome, *et al.* 1993) in that its cortical alveoli are not inflated. It also differs from Ciliophora in that it does not contain a macronucleus.

Flagellate stages were observed for brief periods in senescent cultures of *C. velia*. The flagellates were very short lived and transformed into the spherical immotile form several minutes after their appearance. Accumulation of ultrastructural evidence (such as possible presence of an apical complex) could aid finer taxonomic placement of Chromerida, but requires the successful production and examination of large numbers of these flagellates. In the interim, the organism has been assigned to a new phylum within Alveolata, based on the ultrastructure of the immotile lifestage.

2. Isolation and culturing of *Chromera velia*

Stony corals (Scleractinia, Cnidaria) *Plesiastrea versipora* (Faviidae) from Sydney Harbour, NSW, Australia (animals collected by Thomas Starke-Peterkovic, and Les Edwards, December 2001, alga isolated by R. Moore), and *Leptastrea purpurea* (Faviidae) from One Tree Island Great Barrier

Reef, Queensland, Australia (animals collected by Karen Miller and Craig Mundy, November 2001, alga isolated by R. Moore), were obtained in order to culture the photoautotroph *Symbiodinium*, which is the major intracellular symbiont of these cnidarians[14,15]. A novel brown unicellular alga was also cultured during this process, and this new genus and species has been formally described as *Chromera velia* in the main text. Material presented in the main paper is from type culture RM12, of type host *Plesiastrea versipora*, and type locality Sydney Harbour, Australia. An alternative host is *Leptastrea purpurea*, One Tree Island, Queensland, Australia (data not shown).

Chromera velia was isolated from corals by varying the method of York[16] (1986). Laboratory bleach (NaOCl + NaOH) was neutralized to pH 7.4 using HCl and allowed to sit capped overnight. This was diluted 1:25 in autoclaved seawater and used to surface sterilize the coral nubbins overnight. Tissues were removed from the coral skeletons using a pressurised airstream and then shaken vigorously in a 15 ml capped polypropylene tube to separate animal cells from algal symbionts. Algal cells were pelleted by centrifugation at 3000 rpm for 10 minutes. A cream-white layer of animal derived cell-debris and bacteria covered the brown algal pellet and was loosened by repeated inversion of the tube, before decanting the debris. Autoclaved seawater was added and the process of vigorous shaking, centrifugation, and gentle decanting was repeated until the algal pellet had been purified 6 times and was a dark brown color.

The freshly isolated algal material was serially diluted into 24-well tissue culture plates containing a variant of f/2 medium[17] as follows: 0.5 ml of trace metal stock ($CuSO_4.5H_2O$ 20 mg/L, $ZnSO_4.7H_2O$ 44 mg/L, $CoCl_2.6H_2O$ 22 mg/L, $MnCl_2.4H_2O$ 360 mg/L, $NaMoO_4.2H_2O$ 13 mg/L), 1 ml of 23 g/L FeEDTA, and 0.5 ml of vitamin stock (thiamine HCl 2 mg/L, biotin 10 μg/L, cobalamin 10 μg/L) were added to one litre of autoclaved seawater. Chlorinating agent trichloroisocyanurate (TCIC, Sigma-Aldrich St Louis MO) was dissolved in seawater to saturation, brought to pH 7.7, autoclaved, and then added to the f/2 growth medium at a dilution of 1:10. Antibiotics at final concentrations of 50 μg/ml ampicillin and 50 μg/ml streptomycin were added. Cultures were grown in this medium at 27ºC for one month (5-10 μEinsteins, 14:10hr light:dark) before ‘dilution streaking‘ onto f/2 agar (containing the above antibiotics) and incubation for 1-2 months. Individual colonies were isolated from agar plates and cultured in liquid f/2 with the antibiotics (but no TCIC).

Symbiodinium spp. and *C. velia* grew equally well from extracts of *L. purpurea*, while only *C. velia* but not *Symbiodinium* grew from *P. versipora* extracts. Clonal isolate RM12 of *C. velia* from *P. versipora* was submitted to the North Queensland Algal Culture and Identification Facility, Townsville Queensland, Australia (accession NQAIF136), as well as the Provasoli-Guillard Culture Collection of Marine Phytoplankton, Boothbay Harbor, Maine USA (accession CCMP2878), and the Culture Collection of Algae and Protozoa, Dunstaffnage Marine Laboratory, Oban, Argyll UK (accession CCAP 1602/1). The NQAIF136 culture is maintained in f/2 medium[17] at 25°C. Permanence of photosynthetic function in *C. velia* was indicated by its stability in culture over a five-year period in f/2, containing no organic carbon source, with proliferation dependent upon light.

3. DNA extraction

Genomic DNA, used as template for primer pairs B-N, P and R (Table S1), was extracted from *C. velia* by multiple rounds of freeze thaw in a buffer of 500 mM NaCl, 50 mM EDTA, 100 mM Tris-HCl (pH 7.7). Proteinase K (Qiagen Valencia CA) was then added to a final concentration of 1 mg/ml with incubation at 55°C overnight, and genomic DNA was then extracted using a Qiagen DNeasy kit, with elution of DNA into sterile milli-Q water. Genomic DNA that was used as template for primer pairs A, O and Q, was extracted with phenol and chloroform[18] after cell lysis by 1% SDS and 2% sarkosyl[14] .

4. PCR of genes for phylogeny and confirmation of culture purity

PCR was carried out with extension times of 2-5 min, and amplicons were cloned using the TOPO cloning system (Invitrogen, Carlsbad CA). Sequences were edited using Sequencher software (Genecodes, Ann Arbor MI).

Multiple amplifications of nuclear SSU rDNA for assessment of culture purity

To test whether only a single nuclear genotype was present in an apparent unialgal culture, amplification of nuclear small subunit (SSU) rDNA was deliberately redundant, employing six pairs of PCR primers (Table S1) each amplifying a near full-length gene fragment. One pair of primers (A) has been previously used to amplify nuclear SSU rDNA from alveolates and invertebrates[14,19], while another five pairs (B-F) were universal (provided under NSF AToL project 431185) and were designed to anneal to conserved positions in an alignment of twenty-one diverse

eukaryotic SSU rDNA sequences from GenBank[20]. This pan-eukaryotic alignment contained near full-length SSU sequences from representatives of opisthokonts, microsporidians, amoebozoans, chromalveolates, archaeplastids, euglenozoans, diplomonads and retortomonads. The alignment was supplemented with GenBank sequences from two rhizarians, *Lotharella* and *Thalassicolla,* for greater breadth, before settling on universal primer sequences. Conserved eukaryote-specific bases at the 3' termini of AToL primers F2, R1, R2, and R4, were identified by comparing these to representative eubacterial and archaebacterial SSU rDNA sequences that were present in the original alignment by Barnes *et al*.[20]. End sequencing of 43 nuclear SSU rDNA sequences of *C. velia* that were obtained using primer pairs B-F and *Pfu* Turbo proofreading polymerase (Stratagene, La Jolla CA) showed that unialgal cultures were monospecific. A minimum of 10 sequences were taken from each of three unialgal lines. Allelic gene copies across the dataset differed by no more than 7 bases per kb (Fig. S1). Sequences obtained via primer pair A also matched those obtained from primers B-F. Judging from the homogeneity of all nuclear SSU rDNA sequences we concluded that *C. velia* contains only a single nuclear lineage.

Amplification and assembly of other loci

Eight fragments of nuclear large subunit (LSU) rDNA were amplified using multiple primer pairs G-O[21-24,14] (Table S1), and were assembled using Seqman (DNASTAR, Madison, WI). These formed a single contig with alleles differing to a minor extent, similar to the extent of variation found among the SSU rDNA alleles of this species. The plastid SSU rDNA gene from the novel alveolate was amplified using primer pairs P and Q[25,26], while *psbA* fragments were amplified using primer pairs R-S[27, and this study] (Table S1). Initially, a 409 bp fragment of the *psbA* gene was obtained using universal primer pair R. Subsequently the C-terminal primer was paired with an N-terminal primer that was designed to preferentially amplify alveolate and stramenopile homologs. Primer pair S retrieved a 876 bp sequence. The two *psbA* fragments amplified by primer pairs R and S respectively were of different lengths, but had identical nucleotide sequences in the overlapping region of 409 bp.

5. Phylogenetic analyses

General analyses

Alignments were generated using ClustalX[28]. Nucleotide phylogenetic trees were computed using Maximum Likelihood (ML) and bayesian inference[29,30]. Nucleotide ML trees were calculated using the GTR model for nucleotide substitutions as implemented in PhyML[29] with discrete gamma

distribution in eight variant site categories and one invariant site category (8+1). All parameters (gamma shape, proportion of invariants, and GTR parameters) were estimated from the datasets. Bootstrap support values were computed using the GTR model and 300 replicates. Nucleotide bayesian trees were computed using MrBayes (version 3.1.2) over 3,000,000 generations, under the GTR model with gamma distribution in 8+1 categories. To verify the phylogenetic position of *C. velia*, topology tests were performed using CONSEL[31]. Slow-fast analysis was undertaken in accordance with the method of Brinkmann & Phillipe (1999)[32] as follows. The number of base changes per site was calculated within each accepted taxonomic group using PAUP[33]. Summing up changes across groups we obtained seven (plastid SSU rDNA) and six (nuclear LSU rDNA) evolutionary rate categories respectively, over a greater number of positions. In the slow-fast method, the most variable sites are progressively excluded from an alignment, and an ML tree is derived at each stage.

Specific gene analyses

Nuclear SSU rDNA

The nuclear SSU rDNA gene sequence was obtained from *C. velia* after amplification using primer pair A. It was aligned with available homologous sequences using the dataset published by Kuvardina *et al.* 2002[34] (kindly provided by B. Leander) and phylogenies were computed with PhyML and MrBayes (main paper). Based on the SSU nucleotide tree (Fig. 2c, main paper), two alternative topologies were tested (Fig. 2d, main paper), and alternative placement of *Chromera* with dinozoans was rejected.

Nuclear LSU rDNA

The *Chromera* nuclear LSU rDNA gene sequence from a single unialgal strain, RM12, was merged from sequence reads after amplification by primers L, M and N. An alignment was generated omitting hematozoean sequences to negate long-branch artifacts. The alignment was manually corrected and highly variable regions were removed. Based on the LSU nucleotide tree (Fig. 2a, main paper), two alternative topologies were tested (Fig. 2b, main paper), and alternative placement of *Chromera* with dinozoans was rejected. A slow-fast analysis (Figs S2a and S2b, supplementary material) was also performed.

Plastid psbA *gene*

The *Chromera* PsbA protein was aligned with available homologues in the red-derived lineages (using Megalign, DNASTAR). Apicomplexans do not possess PsbA, a photosystem II protein, and therefore these taxa are absent from the analysis. The *Chromera psbA* gene fragment contained seven instances of the codon UGA, at positions that encode tryptophan by UGG in other photosynthetic organisms (Fig. S3). The UGA codon was accordingly translated to Trp for the purposes of these phylogenetic analyses. Maximum likelihood (ML) and bayesian trees of the PsbA dataset (Fig. 2f, main paper) were computed employing JTT and WAG models for amino acid substitutions respectively. The *Chromera* PsbA sequence branched with those of peridinin dinoflagellates (bayesian posterior probability 0.96) which are a sister group to apicomplexans. Three alternative topologies (Fig. 2g, main paper) were tested for the PsbA tree. Tests of topology 1 (in which *Chromera* PsbA is sister to peridinin dinoflagellate PsbA) confirmed this placement in one test ($pp > 0.95$). Other topologies were not supported in any test.

Encoding of PsbA in the plastid genome, rather than the nuclear genome, is usually the case in diverse algae and plants. For analysies of the UGA-Trp character, we have assumed that the *Chromera psbA* gene is plastid-encoded. Some plastid-encoded proteins of the apicoplast lineage contain the codon UGA-Trp, specifically in the coccidians *Eimeria*, *Neospora* and *Toxoplasma*[35-39]. A UGA-Trp codon in the middle of a gene has not been reported in any plastid of hemosporidians or piroplasmids, although it has been postulated that UGA read-through may occur in hemosporidians at the ends of some genes, in cases where UGA is closely followed by the UAA-Stop codon[35]. Evolutionary analyses concerning the translation of tryptophan from the UGA codon, are presented below with respect to the relevant translation molecules and organelles involved, excluding nuclear apparatus.

Plastid SSU rDNA

The plastid SSU rDNA alignment was manually checked and corrected. In addition to ML and bayesian trees (Fig 2e, main paper), we undertook a slow-fast ML analysis and analysis of LogDet-paralinear distances, because these tools minimise phylogenetic artifacts that are due to evolutionary rate differences. The slow-fast analysis is shown in Figs S4a and S4b.

A region of the plastid SSU rDNA corresponding to stem 34 of the *E. coli* SSU rDNA, was aligned with apicomplexan and protist plastid homologues to assess whether UGA-Trp usage may correlate

to occurrence of UCA (TCA in the GenBank sequences) at either of the two putative UGA acceptor sites of the rRNA (Fig. S5) as hypothesized by Lang-Unnasch and Aiello[35] (1999). At least one of the apicomplexans that uses UGA-Trp lacked the terminator triplet TCA at both sites, and no correlation existed between TCA triplets and UGA-Trp users. The first TCA triplet was well conserved across a wide range of eukaryotic algae that do not use UGA-Trp. Similarly, even though the TCA sequence was rarer in the second triplet than in the first triplet, there were many non-apicomplexans that contained a TCA sequence in the second triplet.

This analysis suggests that UGA-readthrough in apicoplasts and *Chromera* is not facilitated primarily by SSU rRNA acceptor sites. Rather, the analysis is consistent with isopentenylation of UGG-Trp tRNA leading to accumulation of UGA-Trp codons within ORFs[40]. As a "wobble" phenomenon, isopentenylation of UGG-Trp tRNA may allow the translation machinery in this plastid lineage to read both UGA and UGG codons as Trp codons.

Plastid tRNA-Trp

In view of the hypothesis that UGA-Trp codons may have occurred in the common ancestor of all apicoplasts (main paper, Fig. 3), we tested the possibility that the apicoplast tRNA-Trp gene may have been transferred from the apicomplexan mitochondrion. In available apicoplast genome sequences, only one copy of tRNA-Trp gene was found to be present in each case. The tryptophan-specific tRNAs from apicoplasts were aligned with those of other protist plastids, cyanobacteria (the free-living relatives of plastids), protist mitochondria, and alpha-proteobacteria (the free-living relatives of mitochondria), and a phylogenetic analysis was undertaken (Fig. S6). Plastid Trp-tRNAs were found to be monophyletic, and it was concluded that the apicoplast Trp-tRNA is not derived by horizontal transfer from mitochondria. The presence of UGA-Trp codons in a plastid genome is indicated as an apomorphic character for apicoplasts and *Chromera*, but is a metastable character, not possessed by all members.

6. Pigment analysis and photosynthesis

Photosynthetic activity of *C. velia* was measured using Pulse-Amplitude Modulation (PAM). Maximum quantum yield (F_v/F_m) and the photosynthetic parameters electron transfer rate (ETR), photosynthetic efficiency (α), and light adaption index (E_k) were measured using a WaterPAM (Walz, Effeltrich, Germany) following McMinn *et al.* (2005)[41]. *C. velia* was grown under an

irradiance of 70 μmol photons m^{-2} s^{-1}. Dark adapted samples were kept in the dark for 15 minutes prior to measurement. PAM fluorescence indicated that *C. velia* was actively photosynthesising, with a moderate F_v/F_m value (0.259). The culture responded positively to dark adaption (F_v/F_m 0.397). The ETR (light 38.8, dark 49.3) and α (light 0.074, dark 0.056) values were normal for phytoplankton cultures, and E_k values showed that the culture is well adapted to its light environment.

For pigment analysis, aliquots of cultures were filtered onto Whatman (Brentford, Middlesex UK) GF/F filters, frozen in liquid nitrogen, then extracted by sonication in 100% methanol[42]. Chlorophylls and carotenoids were analysed by the method of Zapata *et al*. (2000)[43] using a Waters (Milford, MA) 626 pump, Gilson (Middleton, WI) 233xL autoinjector (with the sample stage refrigerated at 10°C), Waters Symmetry C8 column (150 x 4.6 mm, 3.5 μm packing, at 30.0°C), a Waters 996 diode array detector and an Hitachi FT1000 fluorescence detector (Hitachi High-Technologies Corporation, Tokyo, Japan). Pigments were identified by comparison of their retention times and spectra with those of mixed standards obtained from known cultures[44] that were injected with each batch of samples. The presence of biliproteins was tested by filtering 20 mL of culture onto a 13 mm diameter Whatman GF/F filter and extracting it by grinding and sonication in 1.5 ml 0.1 M potassium phosphate buffer and examining the extract by spectrophotometer.

Unknown pigments from *C. velia* were separated by semi-preparative chromatography on a Phenomenex (Torrance) Luna C8 column (250 x 10 mm, 5 μm packing) using the method of Zapata *et al*. (2000)[43] with a flow rate of 4 ml min^{-1}. Fractions were transferred to methanol using Waters Sep-Pak C18 cartridges and characterized by combined HPLC/UV-Vis/MS/MS using a Waters Alliance 2690 with a 996 diode array detector and a Finnigan (San Jose CA) LCQ ion trap mass spectrometer fitted with an electrospray source. The column used was a Waters Nova-Pak C18 (3.9 x 150 mm), with a mobile phase of 50/50 methanol water ramped to 100% methanol at 10 minutes, and a flow rate of 0.8 ml min^{-1}. Both positive and negative ion spectra were recorded from separate injections, with data-dependent MS/MS spectra acquired from the most intense ion alternating with normal spectra over the range m/z 150 to 900. Only MS data corresponding to the exact elution of the unknown was examined. A needle voltage of 4.5 kV was used, with a capillary temperature of 275˚C and capillary voltage of 22 V. The sheath gas was 80 psi and the collision energy was 30 V. A purified fraction was further analysed by Liquid Secondary Ion Mass Spectrometry (LSIMS) on a

Kratos (Manchester UK) ISQ double focussing magnetic sector mass spectrometer. The liquid matrix employed was *m*-nitrobenzyl alcohol. The primary beam was 10 kV Cs ions, and the sample ions were analysed with the ion source at 5.3 kV. Full scans were acquired over the range m/z 50 to 800 at a resolution of 1000 at 2 seconds per decade. Accurate mass data was acquired by peak matching at a resolution of 7000, using CsI dissolved in tetraethyleneglycol for reference masses. Hot alkaline hydrolysis of the fraction was conducted according to Davies[45]. Unknown pigments were quantitated by assuming their molar extinction coefficients matched those of fucoxanthin or violaxanthin (depending on the spectral shape) and correcting for differing absorption maxima by the method of Wright and Mantoura[46].

HPLC pigment analysis showed that *C. velia* contained chlorophyll *a* and violaxanthin as major components and β, β-carotene as a minor component (Fig. S7, Table S2). No other chlorophylls were detected apart from a trace of what was assumed to be magnesium divinyl pheoporphyrin a5 monomethyl ester (MgDVP). Biliproteins were not detected. *C. velia* contained a single additional unknown pigment (Peak 6, Fig. S7) as the major carotenoid. Positive ion electrospray mass spectrometry of the major carotenoid from *C. velia* gave a clear $[M+H]^+$ ion at m/z 659 as well as a strong ion for the loss of one water molecule at m/z 641, indicating a molecular weight of 658 Da for the unknown pigment. MS/MS product ions from m/z 641 included an intense ion at m/z 581, with this loss of 60 Da indicating the presence of an acetate group. Negative ion data supported this with an $[M-H]^-$ ion at m/z 657, which also gave an MS/MS product ion for the loss of 60 Da at m/z 597. In a separate analysis the $[M+H]^+$ ion at m/z 659 was selected as the precursor, and its product ion at m/z 599 further supported the presence of the acetate group. LSIMS showed a clear $[M]^+$ ion at m/z 658.42167, which corresponds to a composition $C_{42}H_{58}O_6$ (658.42334, accurate to 2.5 ppm). The pigment did not exhibit a hypsochromic shift when acidified, suggesting that it does not contain a 5,6-epoxide group. Its chemical properties resemble those of isofucoxanthin, however the λmax (467.5 nm in methanol) is significantly greater than that of isofucoxanthin (454 nm in ethanol, an equivalent solvent[47]), suggesting that the unknown carotenoid has an extra conjugated double bond in the chromophore. This, coupled with the absence of any fine structure in the visible spectrum, is consistent with a terminal endo-cyclic ketone[48]. Alkaline hydrolysis produced a more polar compound (RT = 15.31 min) with a slightly higher λmax (471.6 nm in eluant) consistent with an acetate ester. The identity of violaxanthin in *C. velia* was confirmed by chromatographic retention time, UV-Vis spectrum, molecular weight (600 Da), and pronounced hypsochromic shift

after acidification from 441 nm to 402 nm. Minor peaks 2 & 5 (Fig. S7) had UV-Vis spectra in methanol virtually identical to the major violaxanthin peak. Likewise the minor peak 3 resembled the major peak 6, suggesting that the minor peaks could be esters of the major carotenoids.

The pigments of *C. velia* are similar to those of the Eustigmatophyte, *Nannochloropsis* sp. (Fig. S8, Table S3), except that unknown peak 6 replaces the vaucheriaxanthin esters, and the violaxanthin is not accompanied by its usual xanthophyll cycle constituents, antheraxanthin and zeaxanthin. *C. velia* peak 2 co-chromatographs with, and has an identical spectrum to *Nannochloropsis* peak 12. *C. velia* peak 6 had an identical spectrum to the minor *Nannochloropsis* peak 19, but eluted earlier.

In the Eustigmatophyte algae[49] such as *Nannochloropsis*, chlorophyll *c* has been lost and chlorophyll *a* retained without degeneration of the autotrophic lifestyle. The retention of a single chlorophyll by *Chromera* is analogous.

7. Light Microscopy

Photography of *C. velia* cells with Nomarski differential interference contrast (Fig. S9) was performed using an Olympus BX51 microscope with an Olympus DP70 camera. A Zeiss Axiovert 40 CFL inverted microscope and a Leitz Labovert inverted microscope, were used for routine observations of the proliferative state and purity of *de novo* cultures under phase contrast (Fig. S10). A Canon Powershot G6 camera was used for routine documentation on the Zeiss Axiovert 40 CFL microscope.

The topmost and middle cells in Figure S9 correspond in division stages to the cells in Figures 1a and 1b, of the main paper, respectively. In the population of cells in Figure S10, many cells contained an accumulation body.

8. Fluorescence microscopy

Living cells were stained with 250 nM (final concentration) MitoTracker® Red CMXRos (Invitrogen, Carlsbad CA) for 2 hours on ice, then centrifuged at 10 000 rpm for three minutes at 4ºC. These cells were subsequently kept on ice at all times. The pellet was retained and the medium discarded. Cells were resuspended in methanol and acetic acid (3:1) for 5 minutes to bleach autofluorescence[50]. The bleaching reagent was then discarded and fresh bleaching reagent added

(repeated 4 times). The tube of cells and bleaching reagent was then incubated at 4°C for three days prior to microscopy.

Mitochondrial staining (Fig. S11) of *C. velia* cells indicated that each nascent daughter cell contains one large mitochondrion of around 1 μm diameter, but that cryptic vesicles of submicrometre diameters also occur in the cytoplasm, becoming more numerous in some cells (e.g. in senescent cells). During cell division, daughter cells contained the large mitochondrion, plus a single smaller area of staining material (Fig. S11aiii). We note that MitoTracker RedCMXRos could react with hydrogen peroxide in peroxisomes or label other vesicles containing higher amounts of thiols.

9. Electron microscopy

Scanning Electron Microscopy

SEM preparation was done using a graded ethanol series and a *t*-butyl alcohol freeze-drying method[51] and micrographs were obtained using a JEOL JSM 7401-F machine (Tokyo).

Chromera velia cells were oblate spheroids in SEM micrographs. The external surfaces of cells are smooth, with a raised ridge that lies around the equator of the cell, and is bisected periodically (Figs. S12 a-b).

Transmission electron microscopy

Specimens grown in liquid culture were plunged into liquid propane and immediately transferred to liquid nitrogen. Freeze-substitution was performed based on the method[52] of Wakefield *et al.* (2000) using Leica (Vienna) EM CFD equipment. Material was transferred to pre-cooled (-90°C) substitution medium containing anhydrous acetone, molecular sieve (pore diameter 3Å, Fluka Chemie, GmbH, Buchs) and 2% OsO_4. The samples were kept at -90°C for 72 hours, at -20°C and 4°C for 24 hours at both temperatures. Between these steps, temperature was increased at 4-5°C/hour. Samples were warmed to room temperature and washed three times in pure anhydrous acetone and embedded in Polybed 812 (Polysciences Inc., Warrington PA). Polymerization was carried out at 60°C for 48 hours. Ultrathin sections were cut on the Ultracut UCT ultramicrotome (Leica Mikrosysteme Gmbh, Austria) using a diamond knife, transferred onto formwar-coated grids, counterstained with uranyl acetate and lead citrate and finally carbon coated. Specimens were

examined by TEM in a JEOL (Tokyo) 1010 at accelerating voltage of 80 kV, equipped with a MegaView III camera (SIS GMBh, Munster).

Cell division in *C. velia* is usually, but not exclusively, binary. The lower cell in Figure S9 corresponds in division stage to the cell triplet in Figure S13. Three-way division products were commonly seen still joined, in TEM (Fig. S13) and LM (Fig. S9). This is believed to be the only form of non-binary division undergone by *C. velia* because focusing through all planes did not reveal any fourth cell. However, triplet cells were not specifically isolated and followed in real time to determine whether a further division may occur while the three cells are still joined.

Before cell division an invagination occurred that terminated at the mitochondrion (Fig. 1a main paper). This became a cleavage furrow during cell division, and halted at the mitochondrion (Fig. S14). Attached to the mitochondrion (Fig. S14) were many large vesicles that stained grey and had texture, implying they may contain carbon storage compounds.

Some variation was observed in organellar arranegment. The development of the plastid (Fig. S15), could involve gradual lengthening and curvature. Presence of a mitochondrial complex (mc) (Fig. S15a) in a very young cell may point to a dynamic mode of mitochondrial ontogeny.

The mitochondrion of *C. velia* was surrounded by two membranes (Fig. S16), as expected, and these data are presented to support the findings of the fluorescence microscopy which indicated that the very large organelle in this species is indeed the mitochondrion. The mitochondrion contained ampulliform, tubular, and lamellar cristae (Figs. S17 a-b).

The *C. velia* plastid was surrounded by four membranes (Fig. S18), though in many places two of the membranes became so closely appressed that there appeared to be only three membranes (data not shown). The periplastidal compartment was present at only one end of the plastid, the end neighbouring the cell apex (as defined in the main paper), and was roughly triangular in cross section ~40 nm x ~130 nm (Fig. S19).

The distinct cone-like plastid of *C. velia* was constrained by one or more cytoplasmic cilia (main paper, Figs. 1a,f,g) extending inward from the apex of the cell (main paper, Figs. 1f-g) to meet the apex of the plastid at the periplastidal compartment. In cross section the cilium was 90 nm in

diameter. The plastid-anchored region of the cilium was attached to the periplastidal compartment, apparently within it (Fig. S20), indicating that some fraction of the cilium architecture may stem from the same secondary endosymbiosis as the plastid. Figure S20 allows several alternative interpretations of the structure of the internal cilium: that it may be axonemal cilium (a '9+2' pattern of microtubules), primary cilium[53] that lacks the central pair of microtubules, or a novel bundling of microtubules.

The alveoli of dividing cells were often greater in number and lesser in length than those in mature cells. In mature cells each alveolus was on average ~650 nm long (data not shown), and alveoli abutted each other with a gap of ~80 nm. In dividing cells alveoli were as short as 250 nm (Fig. S21a), and could abut closely or not at all, implying they are very dyamnic during the cell cycle. Two plasma membranes surrounded young cells, and the space between these was of a similar width to an alveolus thickness (Fig. S21d). The outer membrane was also double in dividing cells (Fig. S21b), the outer and less intact one apparently being the old outer membrane from the pre-division cell, destined for ecdysis. Golgi were commonly observed (Fig. S22).

References

1. International Commission on Zoological Nomenclature, *International Code of Zoological Nomenclature*, 4th ed. (International Trust for Zoological Nomenclature, London, 1999).
2. Adl, S. M. *et al.* The new higher level classification of eukaryotes with emphasis on the taxonomy of protists. *J. Eukaryot. Microbiol.* **52**, 399-451 (2005).
3. Cavalier-Smith, T., Kingdom Protozoa and its 18 phyla. *Microbiol. Rev.* **57**, 953–994 (1993).
4. Brugerolle, G. Apicomplexan parasite *Cryptophagus* renamed *Rastrimonas subtilis* gen. nov. *Eur. J. Protistol.* **39**, 101 (2003)
5. Levine, N. D. The protozoan Phylum Apicomplexa (CRC, Boca Raton, FL USA, 1988)
6. Mehlhorn, H., Peters, W., Haberkorn, A. The formation of kinetes and oocysts in *Plasmodium gallinaceum* and considerations on phylogenetic relationships between Haemosporidia, Piroplasmida, and other Coccidia. *Protistologica* **16**, 135-154 (1980).
7. Levine, N. D. *Perkinsus* gen. n. and other new taxa in the protozoan phylum Apicomplexa . *Parasitology* **64**, 549 (1978).
8. Cavalier-Smith, T., Chao, E. E. Protalveolate phylogeny and systematics and the origins of Sporozoa and dinoflagellates (phylum Myzozoa nom. nov.) *Eur. J.Protistol.* **40**, 185-212 (2004).
9. Cavalier-Smith, T. Cell diversification in heterotrophic flagellates, in *The Biology of Free-living Heterotrophic Flagellates* (eds Patterson, D. J. & Larsen, J.) 113-131 (Oxford Univ. Press, Oxford, 1991).
10. Doflein F. Die Protozoen als Parasiten und Krankheitserreger nach biologischen Gesichtspunkten dargestellt. (Jena, 1901)
11. Silberman, J. D., Collins, A. G., Gershwin, L., Johnson, P. J., Roger, A. J. The ellobiopsid *Thalasomyces* is an alveolate. *J. Euk. Microbiol.* **51**, 246-252 (2004).
12. Bütschli, O. 1885. Dinoflagellata. In Protozoa (1880-1889), in *Bronn's Klassen und Ordnungen des Tierreichs* **1**, 906-1029.
13. Fensome, R. A., *et al*. A classification of fossil and living dinoflagellates. Micropaleontology, Special Paper No. 7, 351 p. (1993)
14. Moore, R.B. Molecular ecology and phylogeny of protistan algal symbionts from corals. PhD Thesis, University of Sydney, Australia. (2006).
15. Rodriguez-Lanetty, M. *et al.* Latitudinal variability in symbiont specificity within the widespread scleractinian coral *Plesiastrea versipora*. *Mar Biol* **138**, 1175-1181 (2001).
16. York, R. H., Jr. Isolation and culture of symbiotic algae, in *Coral Reef Population Biology*, (eds Jokiel, P. L., Richmond R. H., Rogers, R. A.) 486-487 (Hawaii Univ.Sea Grant Coll.Program, Honolulu, HI 1986).
17. Guillard, R. R. L., Ryther. J.H. Studies of marine planktonic diatoms. I. *Cyclotella nana* Hustedt and *Detonula confervacea* Cleve. *Can. J. Microbiol.* **8**, 229-239 (1962).

18. Sambrook, J. Russell, D. W. Molecular Cloning: A Laboratory Manual (Third Edition), Cold Spring Harbor Laboratory Press, New York (2001).

19. Wollscheid, E., Wagele, H. Initial results on the molecular phylogeny of the Nudibranchia (Gastropoda, Opisthobranchia) based on 18S rDNA data. *Mol Phylogenet Evol* **13**, 215-226 (1999).

20. Barns, S. M. *et al.* Perspectives on archaeal diversity, thermophily and monophyly from environmental rDNA sequences. *Proc Natl Acad Sci USA* **93**, 9188-9193 (1996).

21. Lenaers, G. *et al.* Dinoflagellates in evolution. A molecular phylogenetic analysis of large subunit ribosomal RNA. *J Mol Evol* **29**, 40-51 (1989).

22. J. Fehling, J. *et al.* Domoic acid production by *Pseudo-nitzchia seriata* (Bacillariophyceae) in Scottish Waters. *J Phycol* **40**, 622-630 (2004).

23. Wuyts, J. *et al.* The European ribosomal RNA database.*Nucleic Acids Res.* **32**, D101-D103 (2004).

24. Zardoya, R. *et al.* Revised dinoflagellate phylogeny inferred from molecular analysis of large-subunit ribosomal RNA gene sequences. *J Mol Evol* **41**, 637-645 (1995)

25. Obornik, M. *et al.* Notes on coccidian phylogeny, based on the apicoplast small subunit ribosomal DNA. *Parasitol Res* **88**,360-363 (2002).

26. Edgcomb, V. P. *et al.* Benthic eukaryotic diversity in the Guaymas Basin hydrothermal vent environment. *Proc. Natl. Acad. Sci. USA* **99**, 7658-7662 (2002).

27. Moore, R. B. *et al.* Highly organized structure in the non-coding region of the *psbA* minicircle from clade C *Symbiodinium*. *Int J Syst Evol Microbiol* **53**, 1725-1734 (2003).

28. Thompson, J. D. *et al.* The ClustalX windows interface: flexible strategies for multiple sequence alignment aided by quality analysis tools. *Nucleic Acids Res* **24**, 4876-4882 (1997).

29. Guindon, S., Gascuel, O. A simple, fast and accurate algorithm to estimate large phylogenies by maximum likelihood. *Syst Biol* **52**, 696-704 (2003).

30. Huelsenbeck, J. P., Ronquist, F. MRBAYES: Bayesian inference of phylogenetic trees. *Bioinformatics* **17**, 754-755 (2001).

31. Shimodaira, H., Hasegawa, M. CONSEL: for assessing the confidence of phylogenetic tree selection. *Bioinformatics* **17,** 1246-1247 (2001).

32. Brinkmann, H. Philippe, H. Archaea sister group of bacteria? Indications from tree reconstruction artifacts in ancient phylogenies, *Mol. Biol. Evol.* **16**, 817–825 (1999).

33. Swofford, D. L. PAUP*. Phylogenetic Analysis Using Parsimony (*and Other Methods). Version 4. Sinauer Associates, Sunderland, Massachusetts (2001).

34. Kuvardina, O. N. *et al.* The phylogeny of colpodellids (Alveolata) using small subunit rDNA gene sequences suggests they are the free-living sister group to apicomplexans. *J Euk Microbiol* **49**, 498-504 (2002).

35. Lang-Unnasch, N., Aiello D. P. Sequence evidence for an altered genetic code in the *Neospora caninum* plastid. *In.t J. Parasito.l* **29**, 1557-62 (1999).

36. Cai, X., Fuller, A. L., McDougald, L. R., Zhu, G., Apicoplast genome of the coccidian *Eimeria tenella*. Gene. **321,** 39-46 (2003)

37. *Toxoplasma* apicoplast genome sequence: GenBank accession U87145

38. *Toxoplasma* apicoplast genome map. http://roos.bio.upenn.edu/~rooslab/jkissing/toxomap.html

39. Annotation of *Toxoplasma* apicoplast genome-encoded genes. http://www.toxodb.org

40. Ralph, S. A. *et al.* Metabolic maps and functions of the *Plasmodium falciparum* apicoplast. *Nature. Rev. Microbiol.* **2**, 203-216 (2004).

41. McMinn, A. *et al.* Effect of Hyperoxia on the growth and photosynthesis of polar sea ice microalgae. *J Phycol* **41.** 732–741 (2005).

42. Wright, S. W. *et al.* Evaluation of methods and solvents for pigment extraction, in *Phytoplankton pigments in oceanography: Guidelines to modern methods* (eds Jeffrey, S. W. et al.) 261- 282 (UNESCO, Paris, 1997).

43. Zapata, M. *et al.* Separation of chlorophylls and carotenoids from marine phytoplankton: a new method using reversed-phase C8 column and pyridine-containing mobile phases. *Mar Ecol Prog Ser* **195**, 29-45 (2000).

44. Jeffrey, S. W., Wright, S. W. Qualitative and quantitative HPLC analysis of SCOR reference algal cultures, in *Phytoplankton pigments in oceanography: Guidelines to modern methods* (eds Jeffrey, S. W. et al.) 343 – 360 (UNESCO, Paris, 1997)

45. Davies, B. H. Carotenoids, in *Chemistry and Biochemistry of Plant Pigments*, 2nd Edition, Vol. 2, T. W. (ed Goodwin T. W.) 38-165 (Academic Press, 1976)

46. Wright, S. W., Mantoura, R. F. C. Guidelines for collection and pigment analysis of field samples, in *Phytoplankton pigments in oceanography: Guidelines to modern methods* (eds Jeffrey, S. W. et al.) 429-445 (UNESCO, Paris, 1997).

47. Foppen, F. H. Tables for the identification of carotenoid pigments. *Chromatogr Rev* **14**, 133-298 (1971).

48. Bjørnland, T. UV-vis spectroscopy of carotenoids, in *Phytoplankton pigments in oceanography: Guidelines to modern methods* (eds Jeffrey, S. W. et al.) 578-594 (UNESCO, Paris, 1997).

49. Hibberd, D. J. Eustigmatophytes, in *Phytoflagellates. Developments in Marine Biology*, (ed Cox, E. R.) 319–334 (Elsevier, New York, 1980).

50. LaJeunesse T. C., Lambert, G, Andersen, R. A., Coffroth, M. A., Galbraith, D. W. *Symbiodinium* (Pyrrhophyta) genome sizes (DNA content) are the smallest among dinoflagellates *J. Phycol.* **41**, 880–886 (2005).

51. Inoue, T., Osatake, H. A new drying method of biological specimens for scanning electron-microscopy - the tert-butyl alcohol freeze-drying method. *Arch. Histol. Cytol.* **51**, 53-59 (1988).

52. Wakefield, T. S., Farmer, M. A. and Kempf, S. C. Revised description of the fine structure of *in situ* "zooxanthellae" genus *Symbiodinium*. *Biol. Bull*. **199**, 76-84 (2000).

53. Wheatley D. N. Landmarks in the first hundred years of primary (9+0) cilium research. *Cell. Biol. Int*. **29**, 333–339, (2005).

Table S1. PCR amplification of near complete (NC) genes and overlapping partial (OP) gene fragments from *Chromera. velia*

Primer pair & fragment length	Primer	sequence (forward above reverse)	annealling temp°C	gene amplified by primer pair	specificity of primer pair	# of clones sequenced	reference
A (NC)	18A1:	5'-CCTAYCTGGTTGATCCTGCCAGT	50	nuc SSU rDNA	invertebrates &	2	3 14, 8 19
	1800:	5'-TAATGATCCTTCCGCAGGTT			protists		
B (NC)	TOL-F1	5'-SSAYCWGGTTGATYCTGCC	55	"	all protists	3	NSF ATOL
	TOL-R1	5'- WWATGATCCWKCYGCAGGTTCA					project 431185
C (NC)	TOL-F1	5'- SSAYCWGGTTGATYCTGCC	55	"	all protists	10	"
	TOL-R2	5'- WACCTTGTTACGACTTYWVCT					
D (NC)	TOL-F1	5'- SSAYCWGGTTGATYCTGCC	55		all protists	10	"
	TOL-R4	5'- GACGGGCGGTGTGTACAAA					
E (NC)	TOL-F2	5'- SAYCWGGTTGATYCTGCCWG	55	"	all protists	10	"
	TOL-R2	5'- WACCTTGTTACGACTTYWVCT					
F (NC)	TOL-F2	5'- SAYCWGGTTGATYCTGCCWG	55	"	all protists	10	"
	TOL-R4	5'- GACGGGCGGTGTGTACAAA					
G (OP)	D1RF:	5'-ACCCGCTGAATTTAAGCATA	55	nuc LSU rDNA	dinoflagellates	1	10 21
	D3B-R:	5'-ACTTCGGAGGGAACCAGCTAC					11 22 (modified from 10 21)
H (OP)	D1RF:	5'-ACCCGCTGAATTTAAGCATA	55	"	"	1	10 21
	1483R:	5'-GCTACTACCACCAAGATCTGC					"
I (OP)	1308F:	5'-CCGCTAAAGAGTGTGTAAC	55	"	"	1	"
	1973R:	5'-GAGCCAMTCCTTTTCCC					
J (OP)	1888F:	5'-ACCGCATCAGGTCTCC	55	"	"	1	"
	2428R:	5'-CAACAGGGTCCTCTTTCCC					
K (OP)	2219F:	5'-GTGATTTCTGCCCAGTGC	50	"	"	1	"
	2992R:	5'-CCTGTCTCACGACGGTCT					
L (OP)	NLF184	5'-ACCCGCTGAAYTTAAGCATAT	44	"	eukaryotes	2	12 23
	NLR2098	5'-AGCCAATCCTTWTCCCGAAGTTAC					
M (OP)	NLF2075	5'-GTAACTTCGGGAWAAGGATTGGCT	44	"	eukaryotes	2	"
	NLR3535	5'-MRGGCTKAATCTCARYRGATCG					
N (OP)	NLF1105	5'-GGTYAGTCGRTCCTRAG	44	"	eukaryotes	2	"
	NLR2571	5'-CTCAACAGGGTCTTCTTTCC					
O (OP)	ZardF:	5'-CCCGCTGAATTTAAGCATATAAGTAAGCGG	45-50	"	alveolates, inver-	1	13 24, 3 14
	ZardR:	5'-GTTAGACTCCTTGGTCCGTGTTCAAGA			tebrates & fungi		"
P (NC)	APC1:	5'-CAGCAGCMGCGGTAATAC	45	cp SSU rDNA	apicomplexans	3	14 25
	APC2:	5'-ACGGTTACCTTGTTACGACTT					
Q (NC)	U514F	5'-GTGCCAGCMGCCGCGG	45-50	cp SSU rDNA	general	1	15 26
	U1492R	5'-ACCTTGTTACGACTT					
R (OP)	psbAf6	5'-GARCACAACATHYTNATGCAYCC	55	psbA	all algae	1	16 27
	psbAL1	5'-CRTGCATWACTTCCATWCC	55				
S (NC)	psbAU140	5'-ACCGTYTYTAYATCGGTTGGTTCGG	45	"	alveolate &	3	This study
	psbAL1	5'-CRTGCATWACTTCCATWCC	45		stramenopile bias		16 27

Table S2. Pigment content of *Chromera velia*. Peak numbers correspond to those of Fig. S7.

Peak	RT (min)	Maxima in eluant (nm)			%III/II	Identity	Molar ratio : Chl *a*	fg per cell
1	9.28	439	575	628	n/a	MgDVP-like	0.003	0.3
2	10.85	417	441	470	100	Unknown carotenoid 1	0.009	1.0
3	13.12		461		0	Unknown carotenoid 2	0.012	1.5
4	17.19	417	440	470	96	Violaxanthin	0.222	25.3
5	20.18	419	441	471	87	Unknown carotenoid 3	0.013	1.5
6	21.64		470.4		0	Unknown carotenoid 4	0.255	31.9
7	25.41	430		665	n/a	Chl *a* deriv	0.010	1.7
8	26.32	428		660	n/a	Chl *a* deriv	0.016	2.8
9	27.10	429		660	n/a	Chl *a*	1.000	169.4
10	27.54	428		660	n/a	Chl *a* epimer	0.012	2.1
11	29.29		454	479	28	β,β-carotene	0.088	9.0

Table S3. Pigment content of *Nannochloropsis* sp. Peak numbers correspond to those of Fig. S8, but have been identified by retention time and UV-vis spectra only.

Peak	RT (min)	Maxima in eluant (nm)			%III/II	Identity
12	10.41	418	441	470	100	Unknown carotenoid
13	14.10	424	448	474	100	Unknown carotenoid
4	16.979	418	441	470	94	Violaxanthin
14	18.15		471		0	Unknown carotenoid
15	19.96	417	440	470	96	Antheraxanthin
16	22.12	422	445	473	81	Vaucheriaxanthin ester
17	22.54	(429)	454	481	30	Zeaxanthin
18	23.34	421	444	473	80	Vaucheriaxanthin ester
19	23.92		474		0	Unknown carotenoid
20	24.09	421	444	473	82	Vaucheriaxanthin ester
9	27.11	431		661	n/a	Chl *a*
11	29.27		454	479	28	β,β-carotene

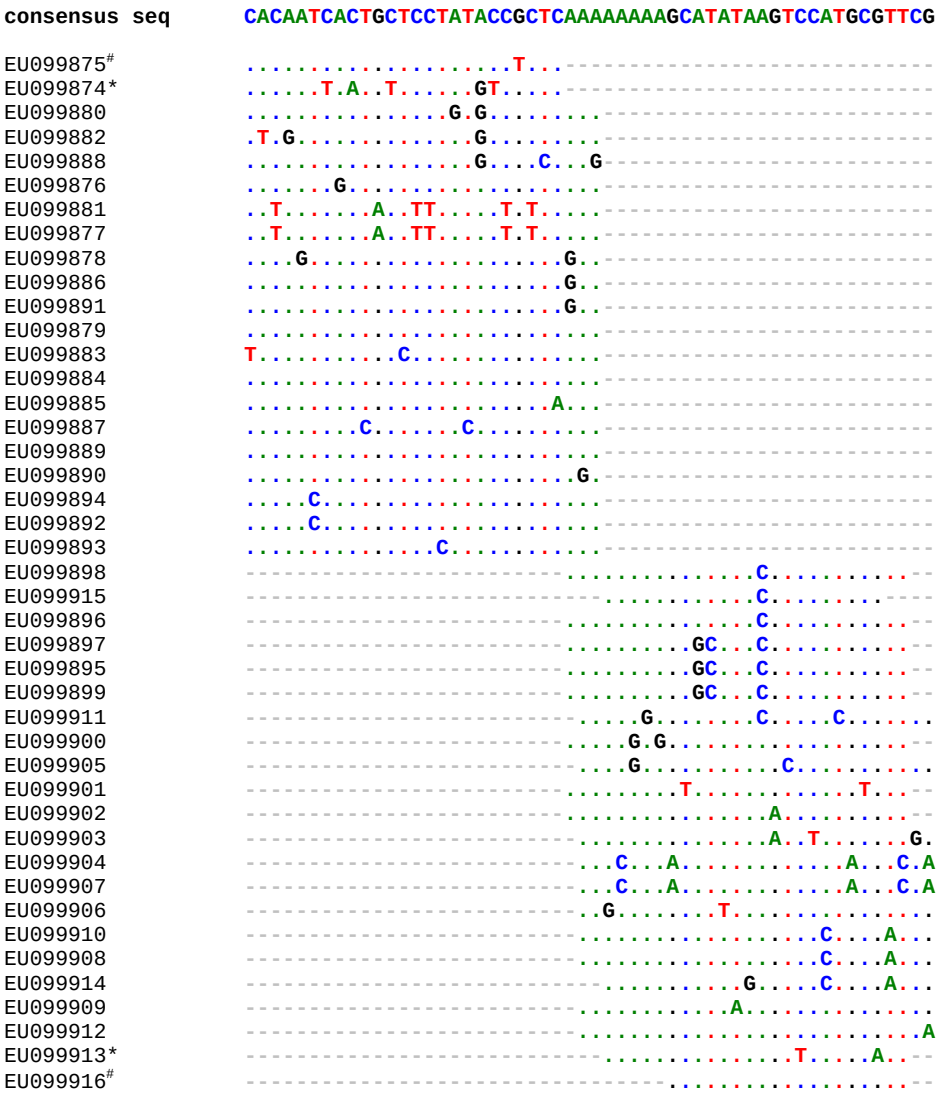

Fig. S1. Purity of *Chromera velia* cultures. End sequencing was performed on 43 nuclear SSU rDNA sequences from 3 cell lines of *C. velia*. The sequences were amplified using primer pairs B-F of Table S1, with the number of repetitions indicated in that table. The alignment is 1720 bases long and only the variable positions are shown (without numbering). Dots indicate identity to the consensus sequence, and dashes indicate unsequenced regions. Hatched sequences are two ends of one molecule (no overlap). Asterisked sequences are two ends of one molecule (no overlap).

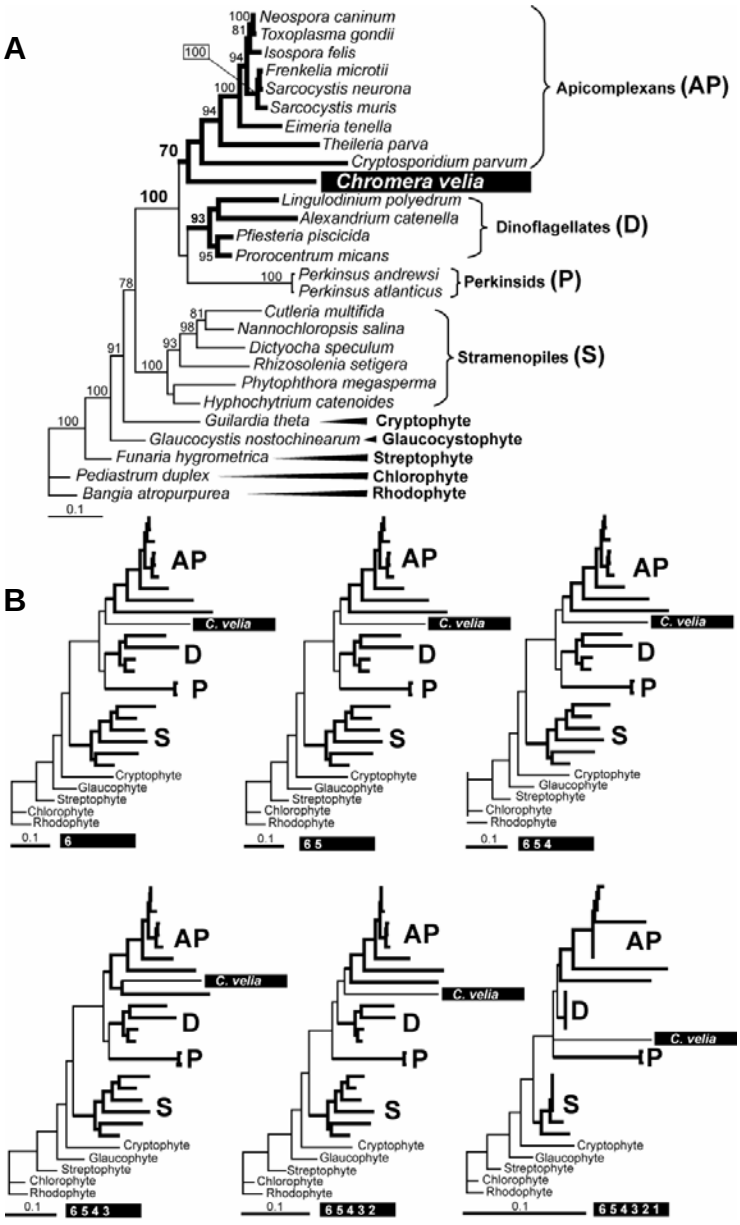

Fig. S2. Slow fast analysis of C*hromera velia* nuclear LSU rDNA (GenBank accession EU106870). (**A**) Abbreviations for groups included in the slow fast analysis (**B**) Slow-fast analysis. The grouping of *C. velia* with apicomplexans is due to fixed characters.

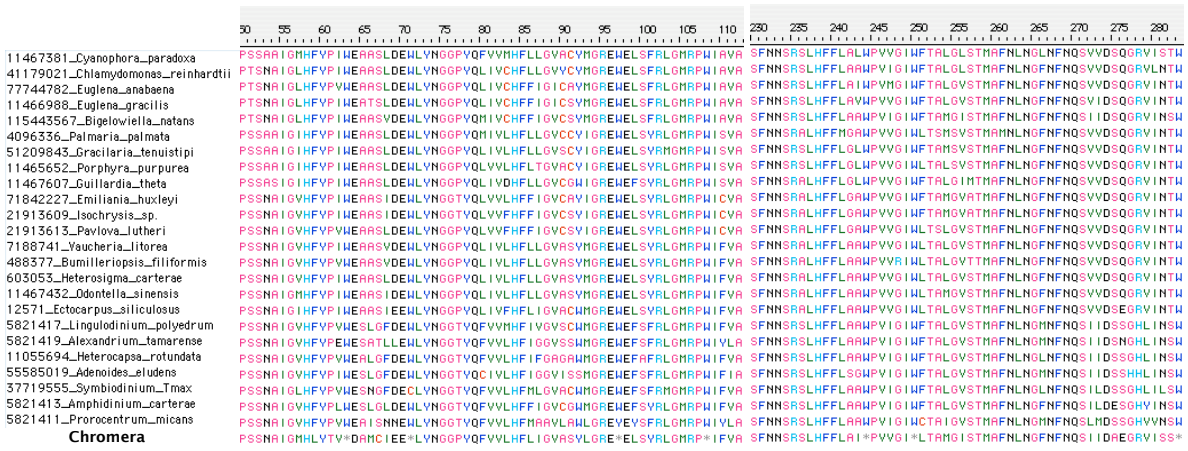

Fig. S3. Amino acid alignment of PsbA sequences from red and green algal lineages. Tryptophan (W) is well conserved at positions 63, 71, 97, 108, 244, 250, and 283. The portion of the protein presented is the portion sequenced. Amino acids between sites 113 and 230 are not shown as they do not include conserved tryptophan sites. The sequenced fragment covers ~83% of the full protein and contains no regions of variable length. *Chromera velia* UGA codons are denoted by an asterisk. GenBank accessions accompany species names. Representaed on the alignment are glaucophytes, chlorophytes, euglenophytes, chlorarachniophytes, cryptophytes, haptophytes, stramenopiles, and dinoflagellates. *C. velia psbA* has GenBank accession EU106869.

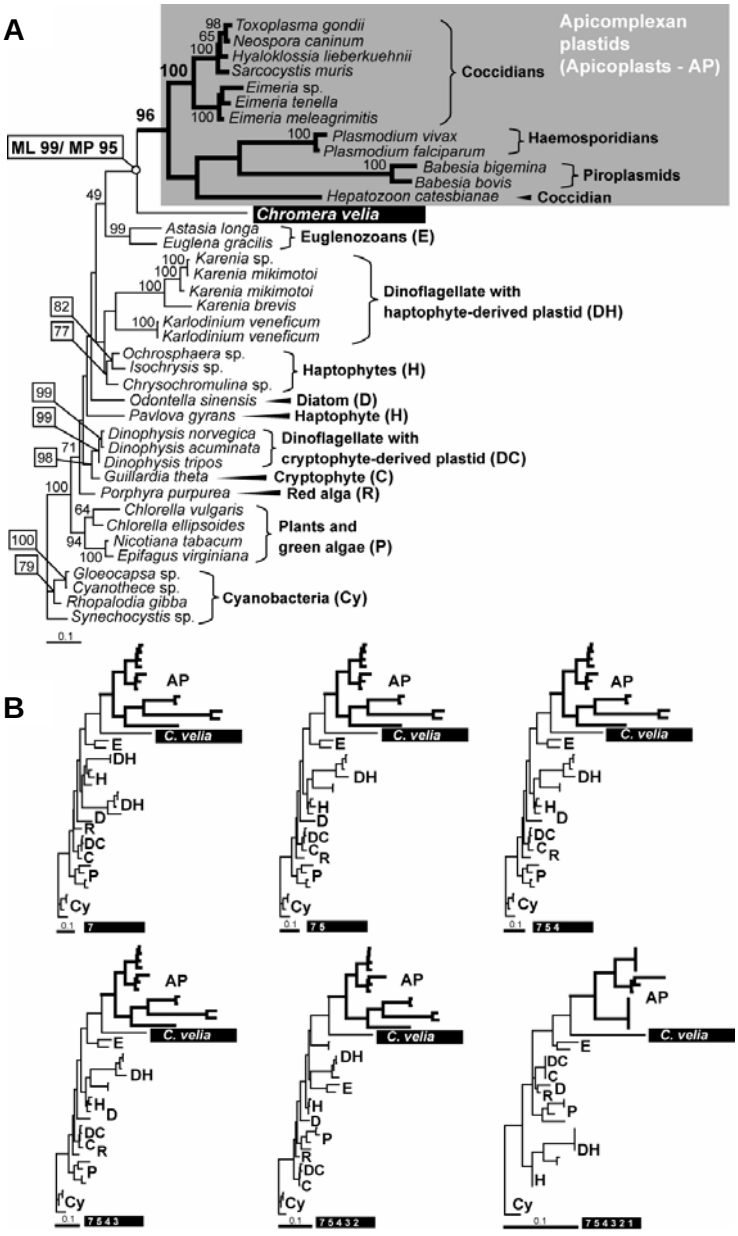

Fig. S4. Slow-fast analysis of *Chromera velia* plastid SSU rDNA phylogeny. (**A**) Abbreviations for groups included in the slow-fast analysis. (**B**) Slow-fast analysis. The grouping of the *Chromera* plastid with apicoplasts is due to fixed characters (GenBank accession EU106871).

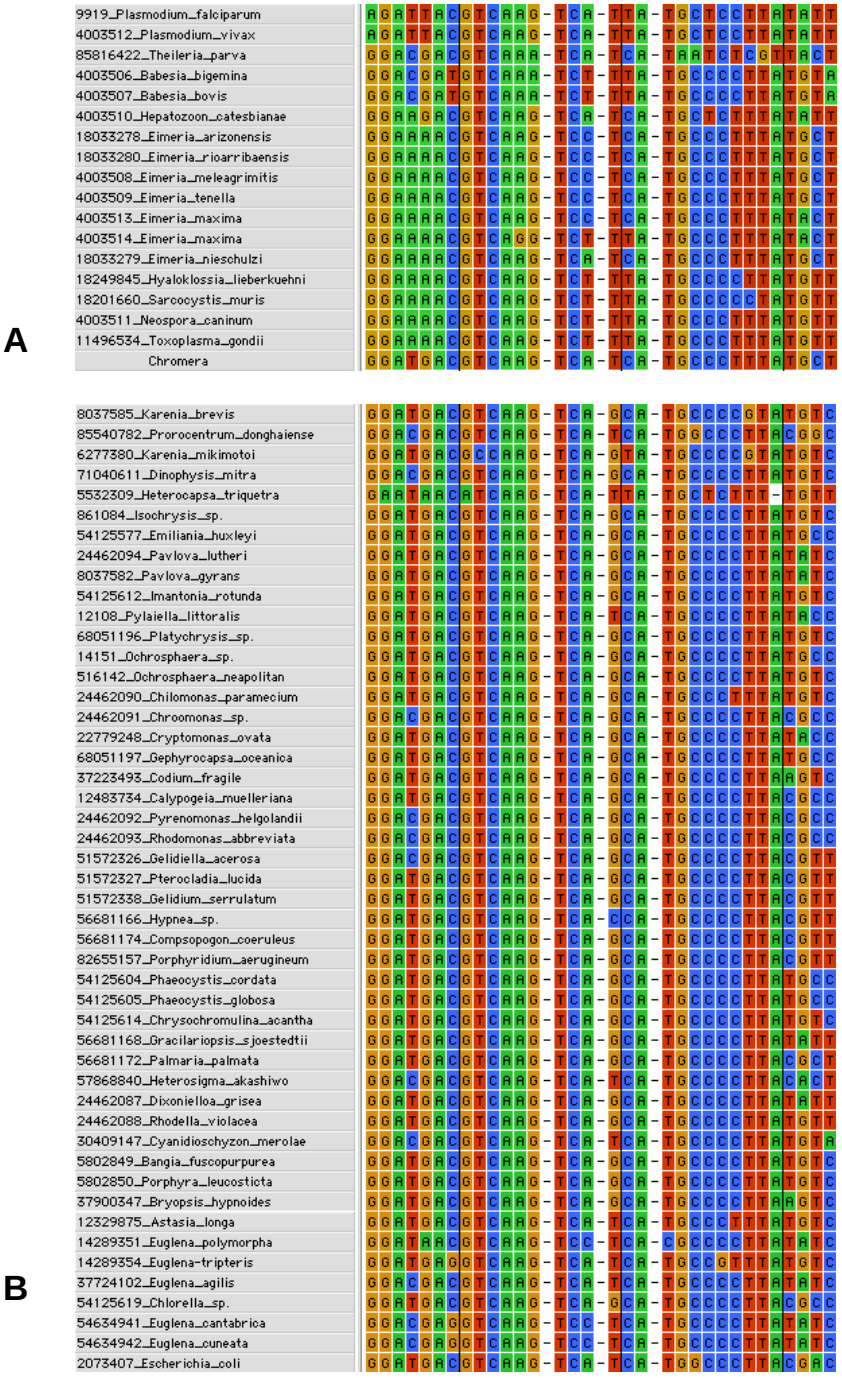

Fig. S5. Putative UGA-binding triplets for tRNA-Trp in plastid SSU rDNA. The two putative UGA terminator binding triplets[35], TCA TCA, (UCA UCA) are separated from flanking sequences by a gap. (**A**) Apicomplexans and *C. velia*. (**B**) Other unicellular algae with *Escherichia coli* 16S SSU rDNA (bottom line) as a comparator[35]. Sequence numbers are GenBank identifiers.

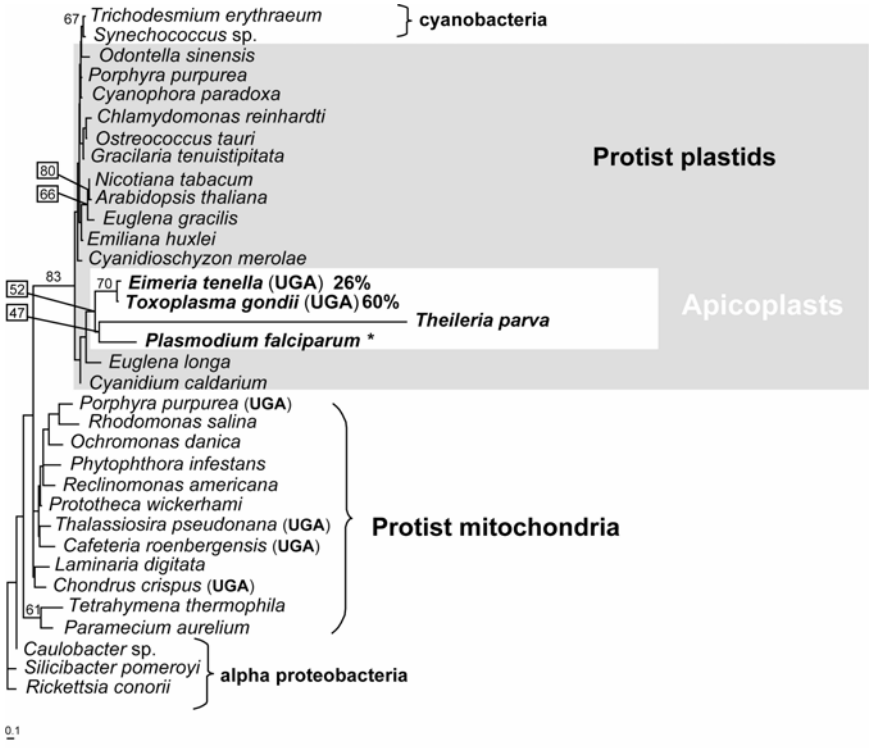

Fig. S6. ML phylogeny of tRNA-trp from apicoplasts, chloroplasts and mitochondria. Plastids and mitochondria that contain UGA within some ORFs are noted. **Plasmodium* is hypothesized to read through UGA if it occurs at the end of an ORF and is closely followed by a UAA Stop codon[35].

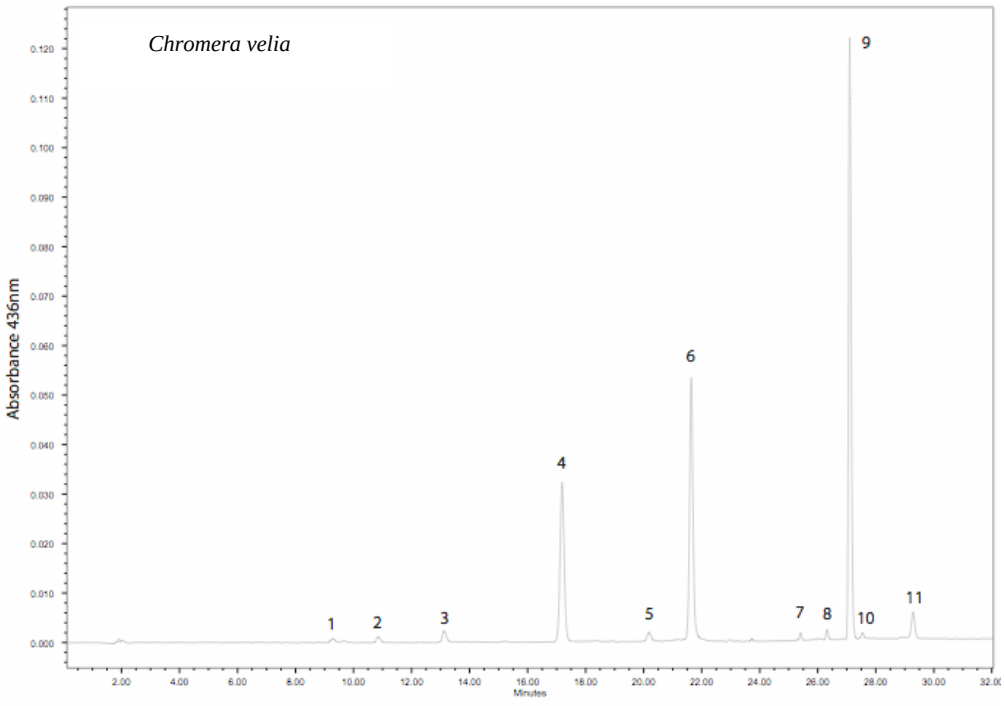

Fig. S7. HPLC chromatogram of pigments obtained from C*hromera velia*

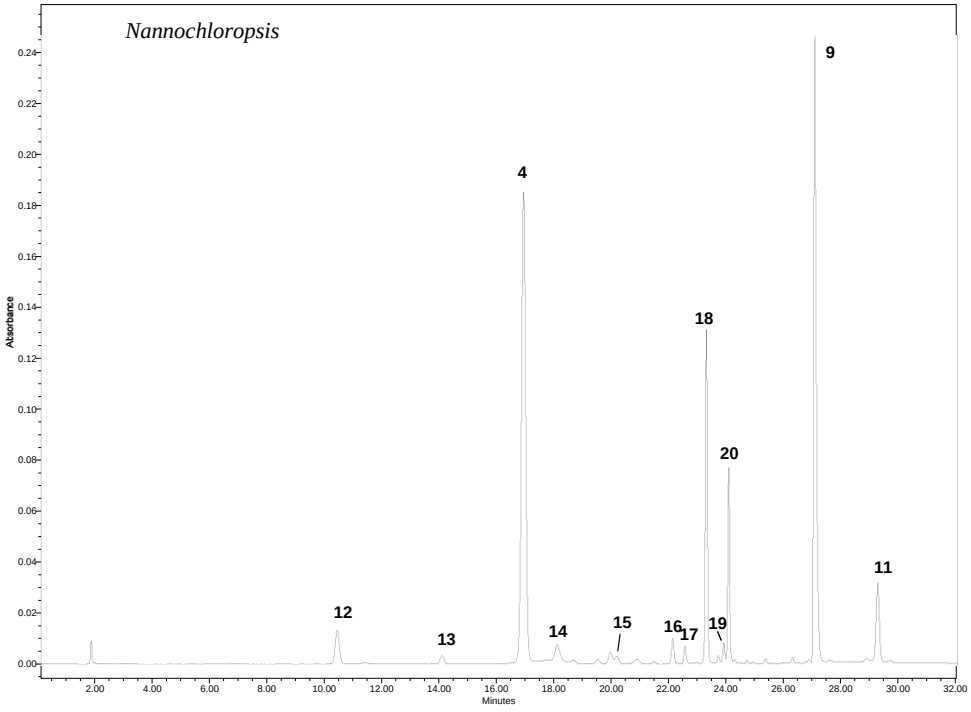

Fig.S8. HPLC chromatogram of pigments obtained from *Nannochloropsis sp.*

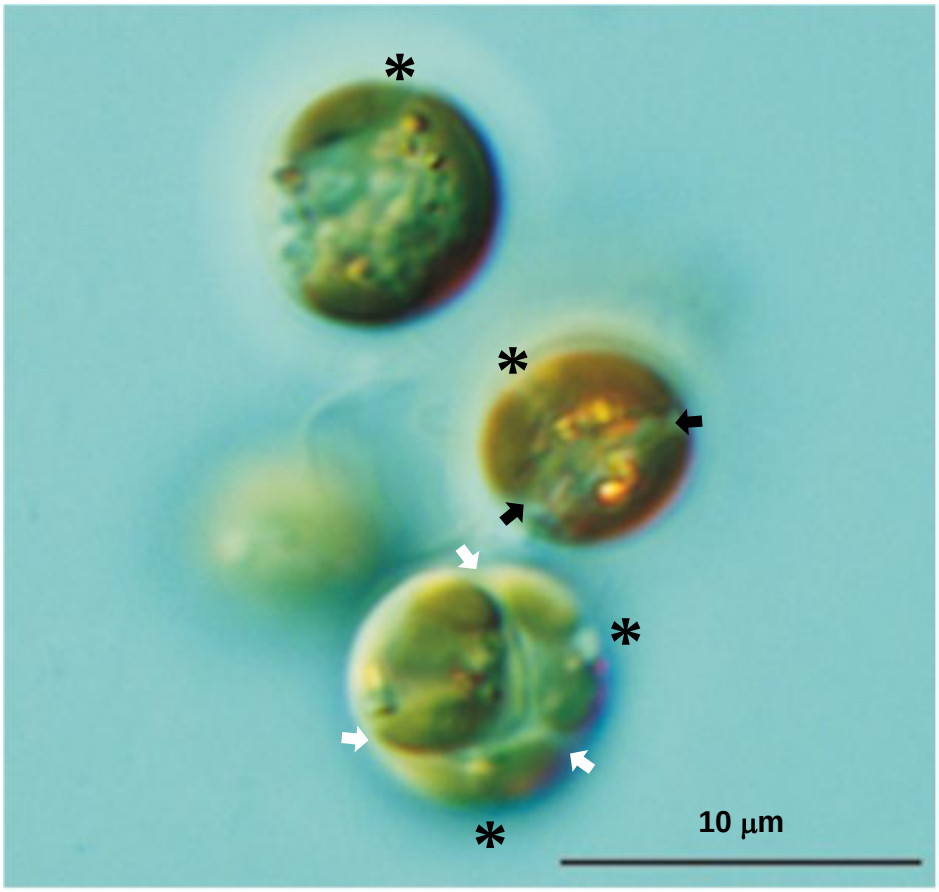

Fig.S9. *Chromera velia* cells during interphase, binary divison, and three-way division. Asterisks indicate the apex of the cell where the apex of the plastid is anchored to the cell periphery. Binary division: black arrows indicate cleavage furrow. Three way division: white arrows indicate cleavage furrows (bar 10 µm).

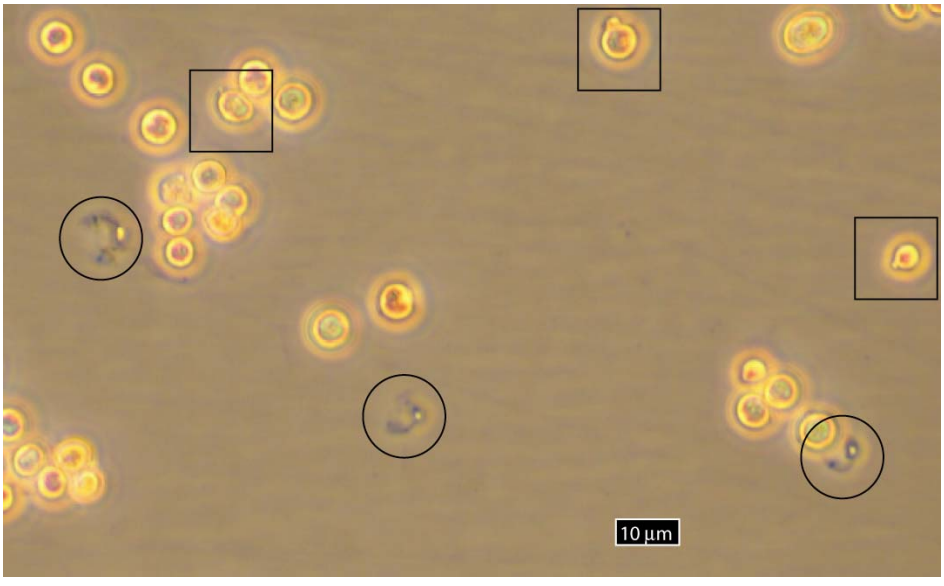

Fig.S10. Accumulation body observed in the cell wall in some *Chromera velia* cells, under phase contrast. Live cells (squares) with accumulation bodies. Discarded outer membranes or cell walls (circles) after cell division or death, still bore the accumulation body (bar 10 µm).

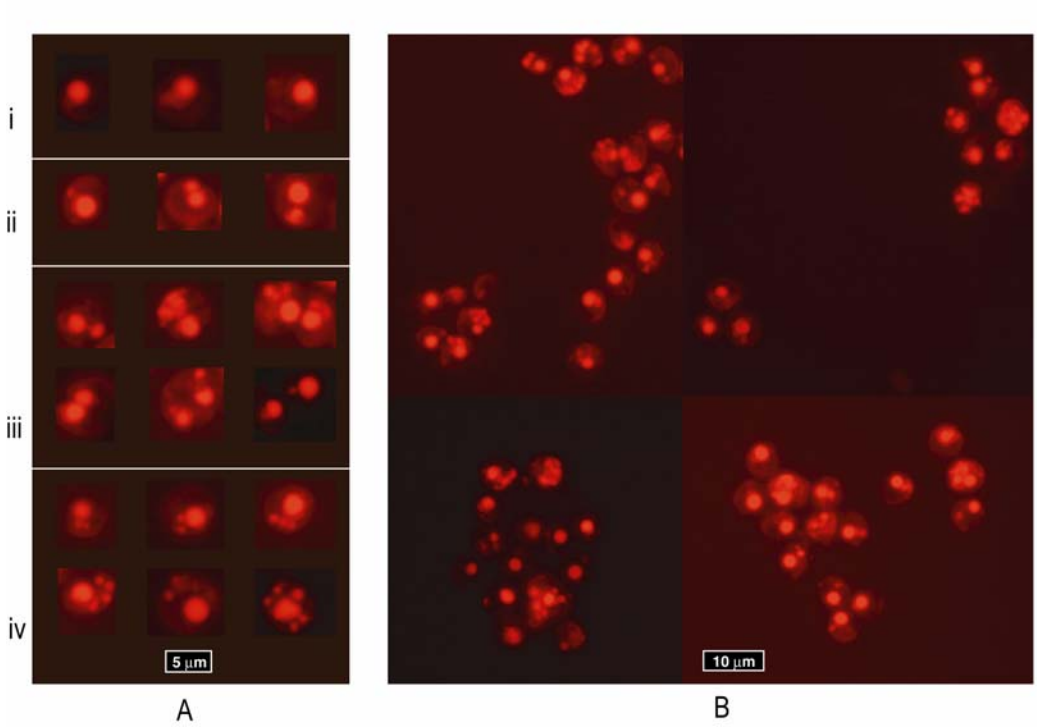

Fig.S11. Mito-red staining of *Chromera velia*. (**A**) Individual cells grouped according to number of objects within a cell that stained with mito-red: (i) Single large mitochondrion (ii) Large mitochondrion with a single smaller object also stained (large objects that stained were possibly sibling organelles, i.e. in preparation for cell division); (iii) Cells dividing. The large mitochondrion of each daughter cell was often accompanied by one or two small objects that stained positively; (iv) Cells generally older and larger than in i and ii, that had developed numerous objects that stained positively. These cells may have been senescent (bar 5 μm). (**B**) Typical populations of cells in four fields. Cells that had a single large mitochondrion, or a large mitochondrion near the cell centre plus a faint-staining object on the edge of the cell, were typical for this species (bar 10 μm).

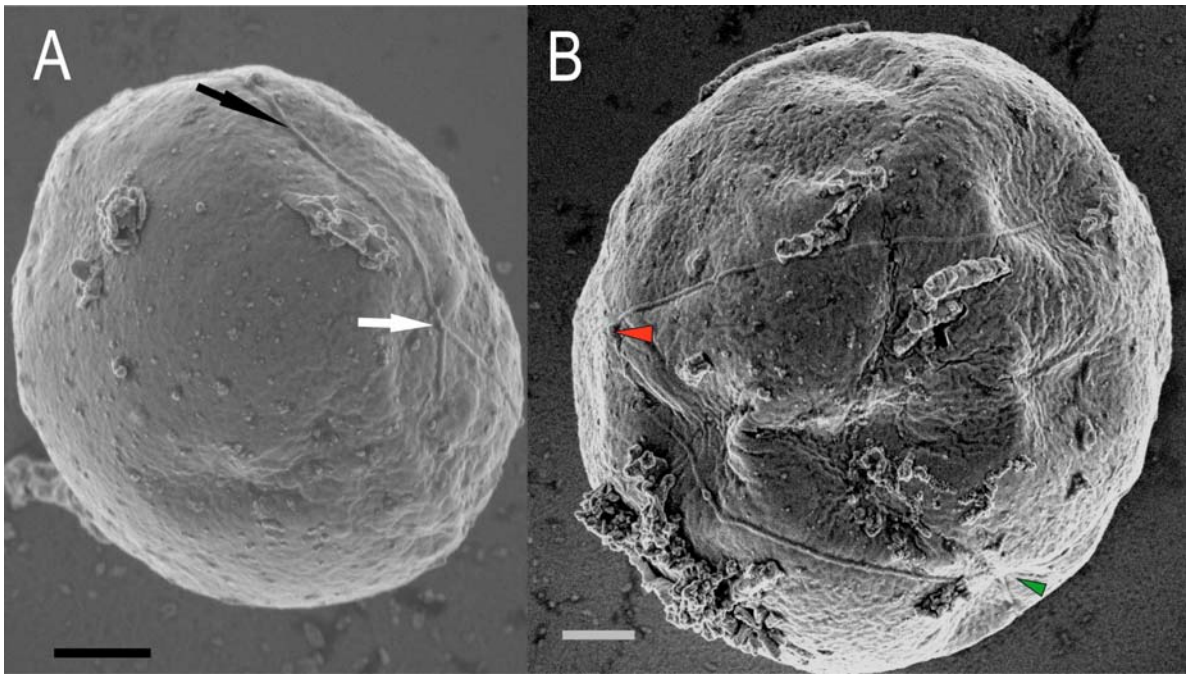

Fig.S12. Scanning electron micrograph of the *Chromera velia* cell surface (**A**) A raised ridge (black arrow), was forked (white arrow) (bar 1 μm). (**B**) A forked ridge (green triangle) also intersected another ridge (red triangle) (bar 1 μm).

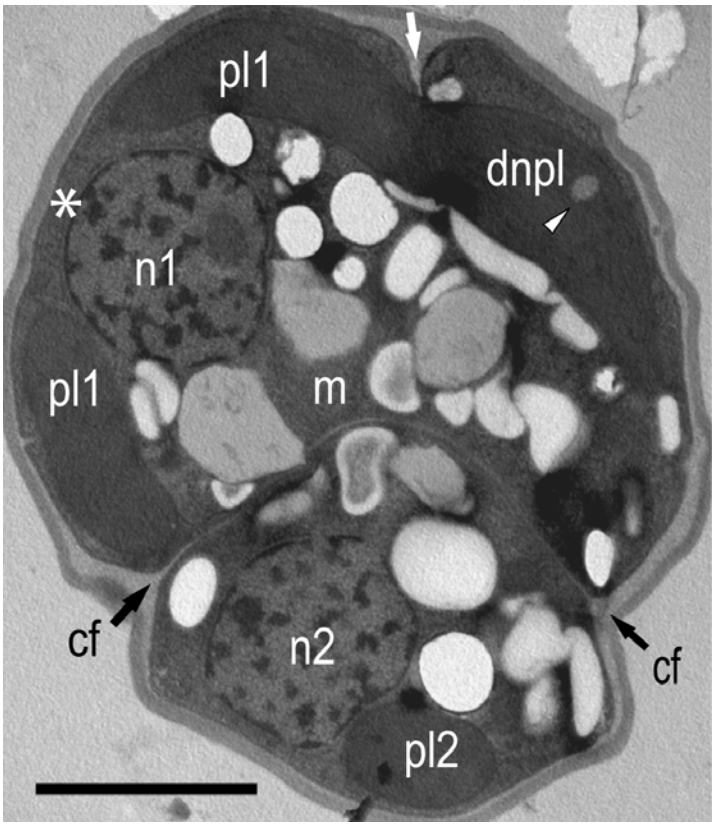

Fig.S13. Cell undergoing multiple division. The parent cell (n1, pl1) divided once at the cleavage furrow (cf) to form the daughter cell (n2, pl2) then began to divide again at a separate cleavage furrow (white arrow) to begin forming a third cell, here including the developing new plastid lobe (dnpl) (bar 2 μm).

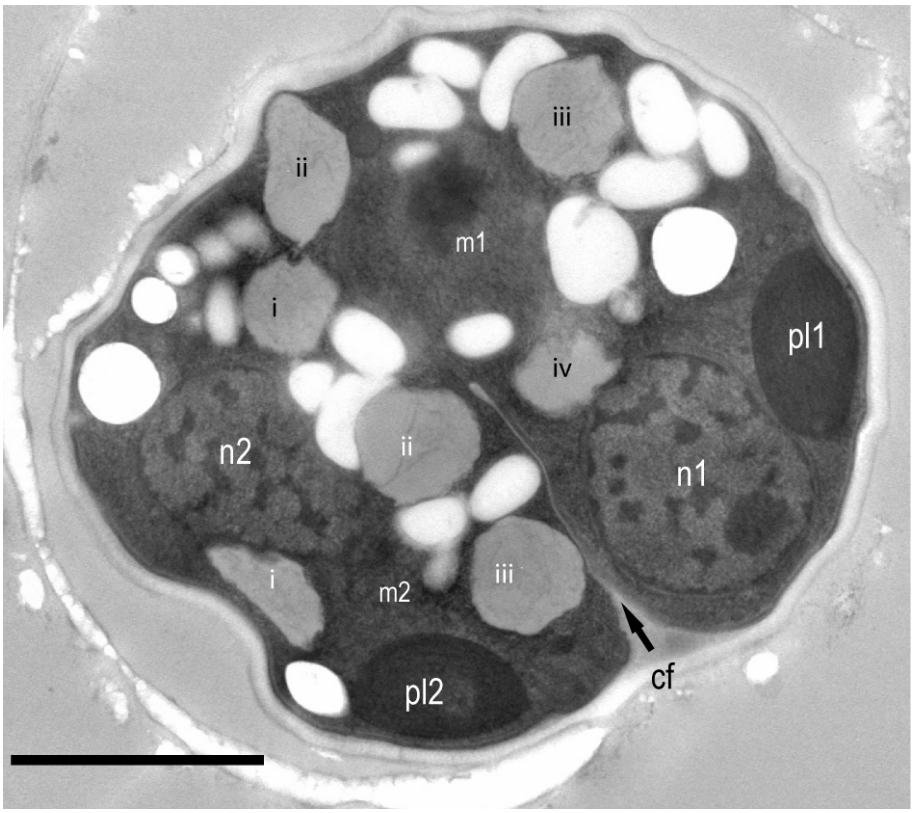

Fig.S14. Formation of the cleavage furrow in *Chromera velia* undergoing binary division. The cleavage furrow (cf) separated nuclei (n1, n2) of nascent parent and daughter cells. The furrow halted at, or circumscribed around, the mitochondrion (m1) of cell 1. The mitochondrion was surrounded by presumptive carbon storage granules (black letters i-iv), which are grey-staining. Nascent cell 2 also contained a mitochondrion (m2) that was also surrounded by carbon storage granules (white letters i-iii). Plastids (pl1 and pl2) were sectioned through their narrowest part (bar 2 μm)

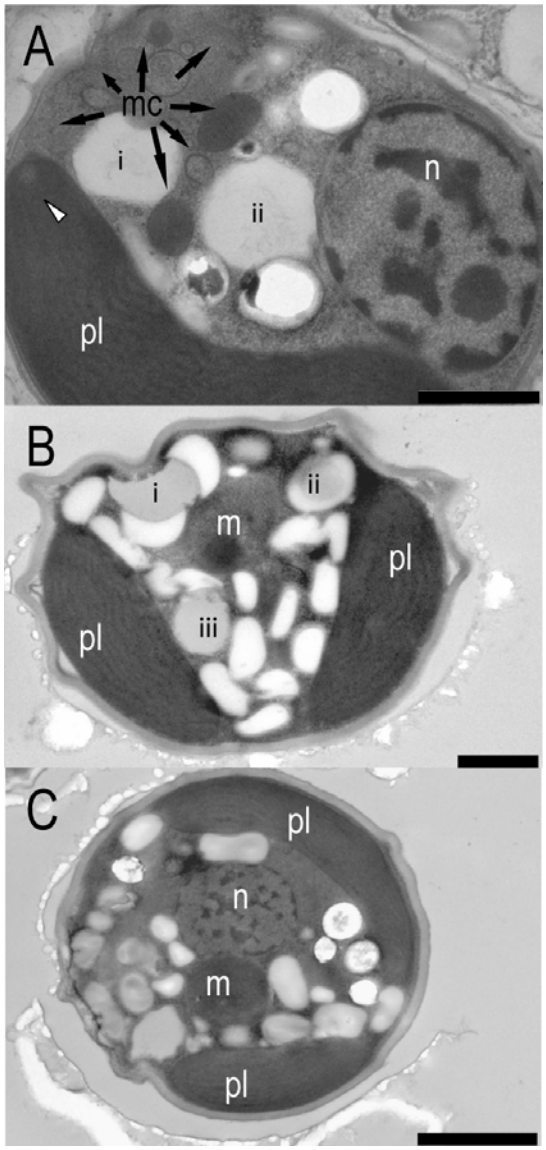

Fig. S15. Conformation of *Chromera velia* organelles at three successive stages of maturation. (**A**) Conformation of plastid in a young cell. In this cell, the mitochondrion had a dynamic structure, a mitochondrial complex (mc), which was the exception rather than the rule. The image is enlarged relative to B-C to show the mc. Presumptive carbon storage granules (i-ii) flanked the dark staining areas of the mitochondrial complex (bar 1 μm). (**B**) Conformation of the plastid in a cell of medium age. The mitochondrion (m) had two distinct compartments, one dark staining the other grey staining and containing membranes. Presumptive carbon storage granules (i-iii) surrounded the mitochondrion (bar 1 μm) **C.** Conformation of the plastid in a mature cell. This was the maximum extent of plastid coverage in this species. In all figures are shown nucleus (n) and plastid (pl) (bar 2 μm).

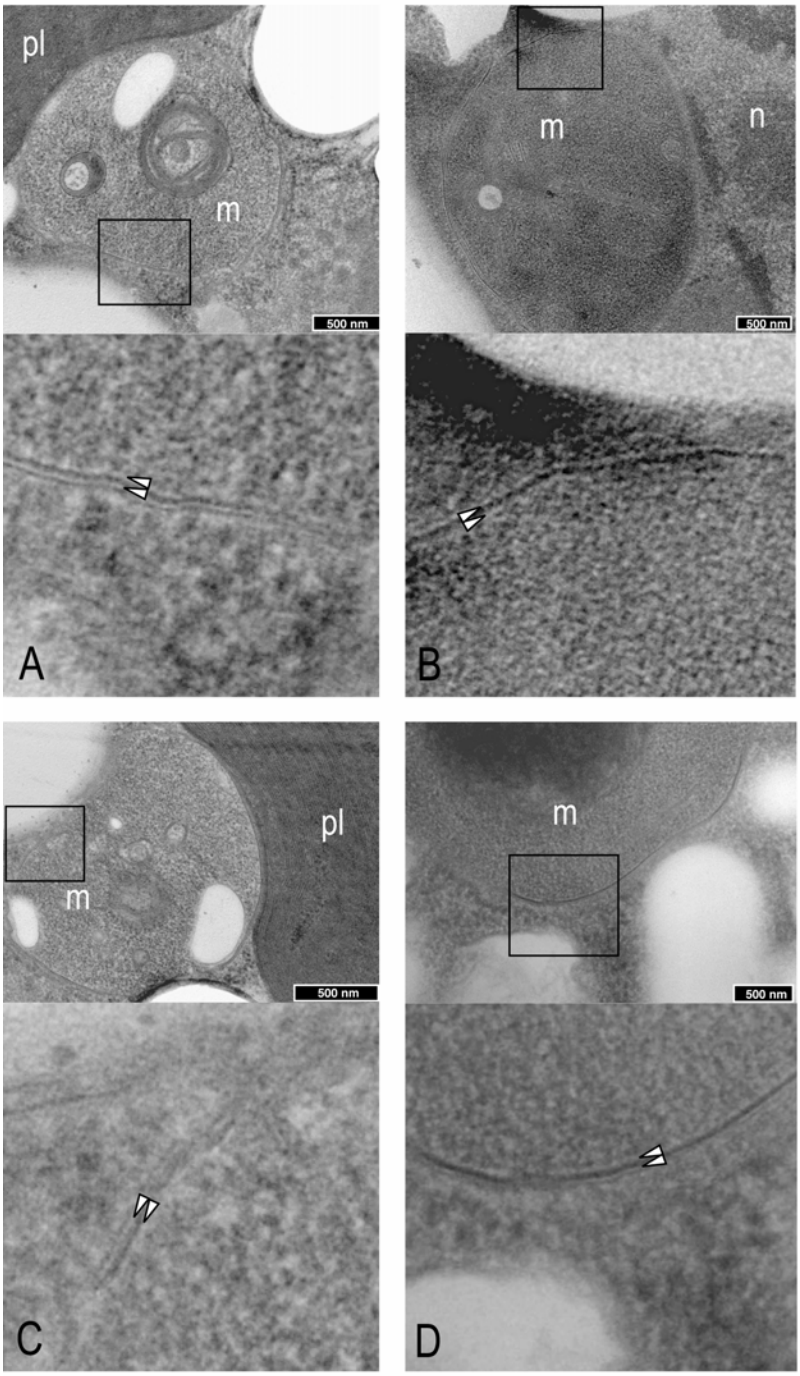

Fig.S16. A double membrane surrounded the *Chromera velia* mitochondrion. Four magnified views (**A-D**) of mitochondria with two membranes (triangles). The lower one of each pair of panels shows a magnified region from the panel above it (black unfilled squares) (bar 500 nm). All views show mitochondrion (m); some show the plastid (pl) or nucleus (n) (bar 500 nm).

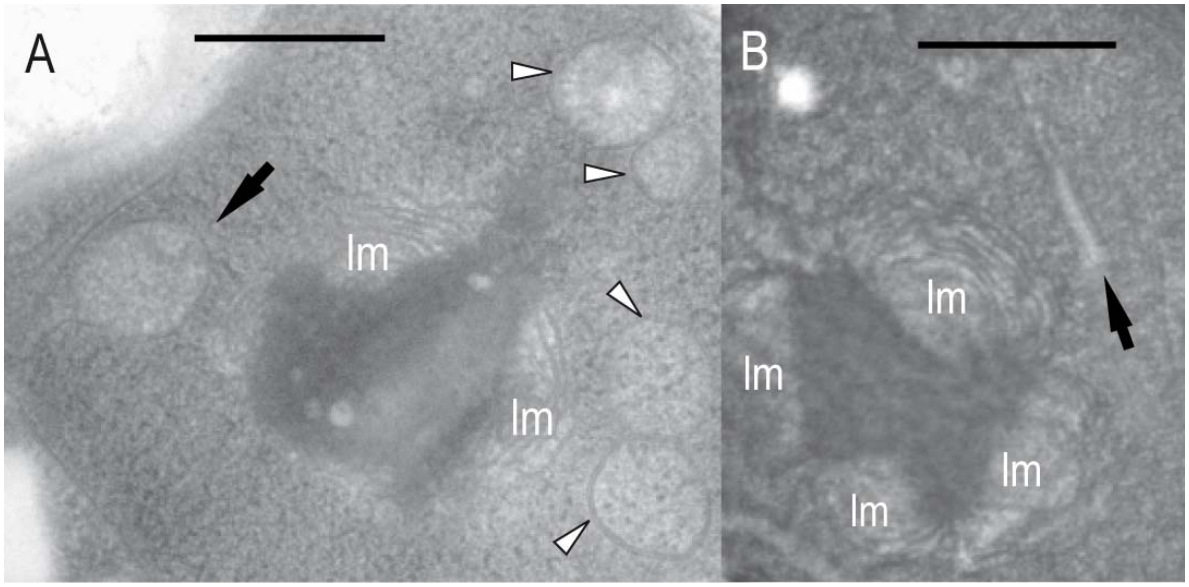

Fig.S17. The internal structure of the mitochondrion. (**A**) It is bilaterally symmetric, and contains ampulliform cristae in transverse section (black arrow) and cross section (white triangles), as well as a lamellar membrane system (lm) (bar 500 nm). (**B**) Tubular mitochondrial cristae (black arrow) were occasionally observed. The lm are arranged symmetrically (bar 500 nm).

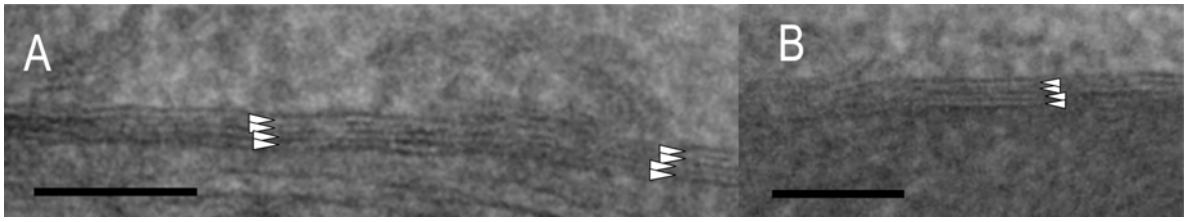

Fig.S18. Number of membranes surrounding the *Chromera velia* plastid. (**A**) Four membranes surrounded the plastid (bar 100 nm). (**B**) A separate cell (than A) also displayed four membranes around the plastid (bar 100nm).

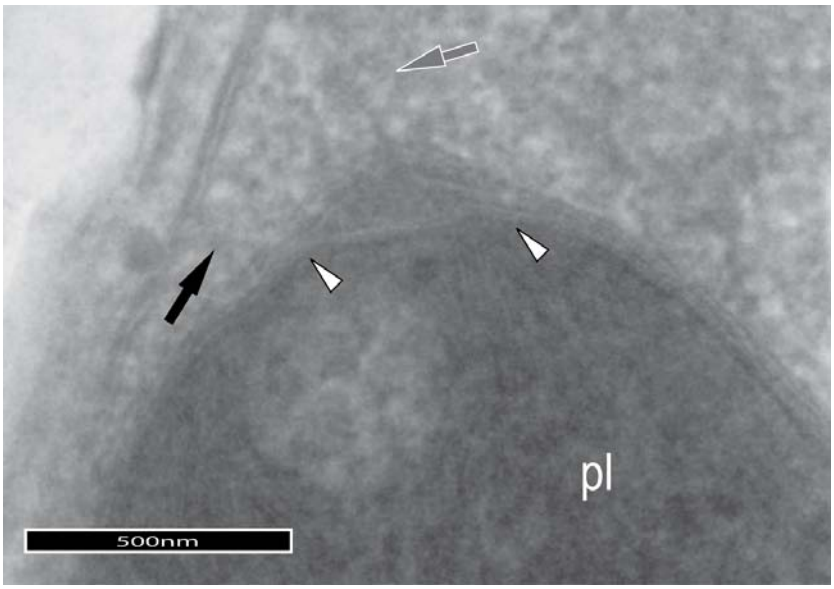

Fig.S19. Periplastidal compartment of *Chromera velia*. The apex of the plastid (pl) was near the apex of the cell (direction of top of frame). The apex of the plastid appeared tethered to the periphery of the cell via a fine filament (black arrow). The filament terminated at a localised dark staining region of the cell wall. Also at the apex of the plastid, the inner pair of membranes that surrounded the plastid were separted from the outer pair (at the white triangles) by the periplastidal compartment that was triangular in section. The periplastidal compartment terminated at a 90 nm diameter object in cross section (grey arrow), best resolved in Fig. S20 below (bar 500 nm).

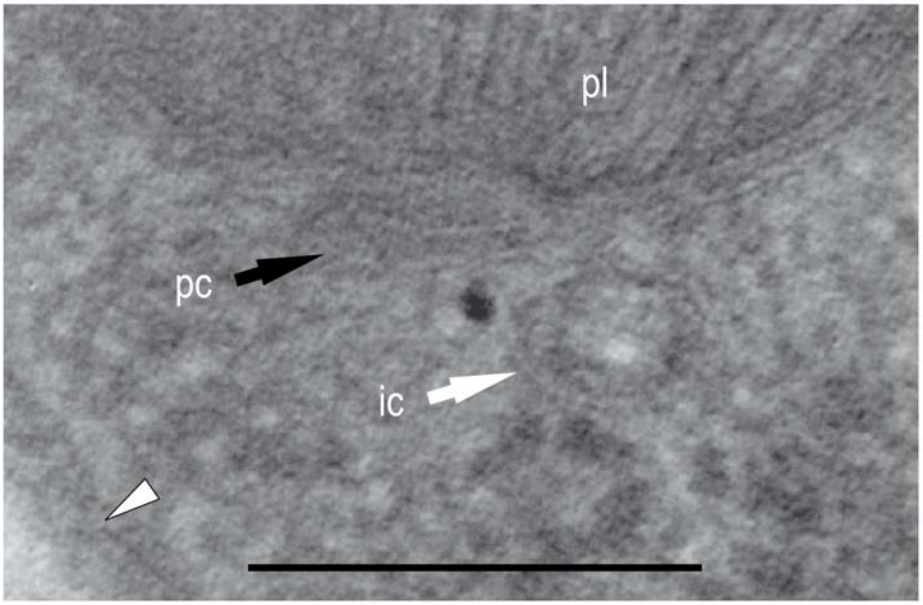

Fig.S20. Cross section of internal cilium (ic, black arrow). The periplastidal compartment (pc, black arrow) is membrane bound and proximal to the cell periphery (white triangle) (bar 200 nm). Microtublues are visible inside the cilium.

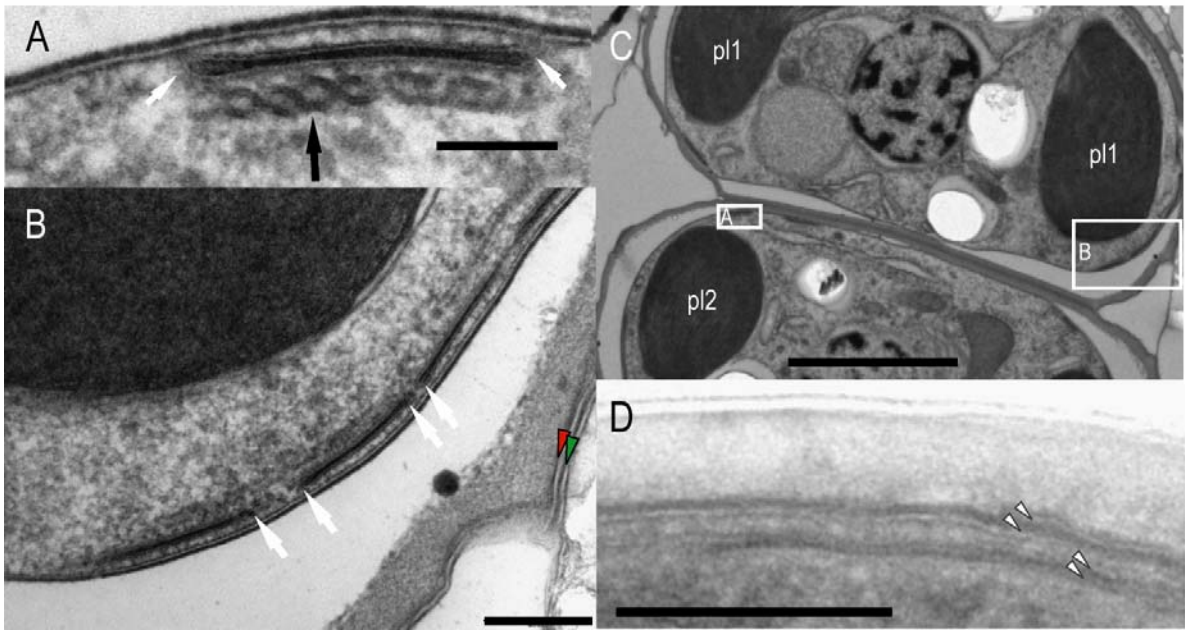

Fig.S21. Alveoli, plasma membrane and outer membrane of *Chromera velia*. Figures A and B are details of C. (**A**) Alveoli and subsurface microtubules. Each alveolus terminated with a slight bulge at both ends (black arrows). Alveoli were underlain by microtubules (white arrow). This alveolus was far from other alveoli because it was very young, occurring near the division site in a dividing cell (bar 100 nm). (**B**) Alveoli abutted each other (white arrows). The outer membrane (green triangle) of the mother cell is being replaced by the outer membrane of the new daughter cell (red triangle) (bar 200 nm). (**C**) Binary division with orientation of plastids (pl1 and pl2) in daughter cells. The cell apices pointed away from the division site (bar 2 μm). (**D**) Two plasma membranes (white triangles) were observed. The thickness of an alveolus (lower pair of white triangles), mirrored the thickness of the space between the two plasma membranes (upper pair of white triangles) (bar 200 nm).

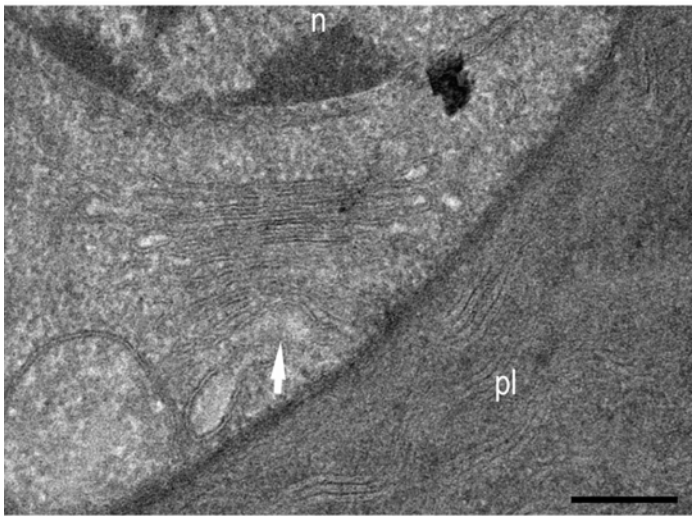

Fig.S22. Golgi apparatus of C*hromera velia*. The cis face of the Golgi stack was always found facing the nucleus, while the trans face generally faced the plastid or was at right angles to the plastid surface (bar 200 nm)